

# **MODELING OF WAX DEPOSITION IN A CRUDE OIL CARRYING PIPELINE**

by

Preston Montalvo

A thesis submitted to the faculty of  
The University of Utah  
in partial fulfillment of the requirements for the degree of

Master of Science

Department of Chemical Engineering

The University of Utah

May 2012

Copyright © Preston Montalvo 2012

All Rights Reserved

# The University of Utah Graduate School

## STATEMENT OF THESIS APPROVAL

The thesis of Preston Montalvo  
has been approved by the following supervisory committee members:

<u>Milind Deo</u>	, Chair	<u>3/21/2012</u> Date Approved
<u>Jaye Magda</u>	, Member	<u>3/21/2012</u> Date Approved
<u>Rich Roehner</u>	, Member	<u>3/21/2012</u> Date Approved

and by JoAnn Lighty, Chair of  
the Department of Chemical Engineering

and by Charles A. Wight, Dean of The Graduate School.

## **ABSTRACT**

The oil modeled in this thesis has a large amount of paraffin and must be transported from where it is extracted to a refinery over a distance that includes changes in elevation and temperature. This study investigated the deposition that would occur due to the paraffin in the oil. In this study the paraffin containing oil was mixed with a diluent in order to lower the wax appearance temperature (WAT) of the oil for one case. The second case involved mixing the paraffin containing oil with a light crude oil that did not contain a large amount of paraffins. The cases were modeled using the DepoWax module found in the commercially available software PVTsim, by Calsep International Consultants. Both of the cases were modeled in a pipeline, when the weather would be the coldest due to the ambient temperature being much lower than the WAT. The large temperature gradient in the pipeline to the outside air causes the temperature of the oil to drop below the WAT and pipeline pressure to be quite high. High Temperature Gas Chromatography (HTGC), viscosity measurements and Fourier Transform Infrared Spectroscopy (FTIR) were used to characterize the oil. The HTGC gave the carbon number distribution of the paraffin containing oil as well as the diluent. Viscosity measurements gave rheological values for the oil at different temperatures as well as different dilutions with the diluent. The FTIR was used to determine the wax appearance temperature (WAT). The measured values from the previous tests all were used as inputs to DepoWax to characterize the oil and the mixtures to be modeled in the pipeline.

## CONTENTS

<b>ABSTRACT.....</b>	<b>iii</b>
<b>NOMENCLATURE.....</b>	<b>vi</b>
<b>ACKNOWLEDGEMENTS .....</b>	<b>x</b>
<b>INTRODUCTION .....</b>	<b>1</b>
<b>LITERATURE REVIEW OF WAX DEPOSITION.....</b>	<b>4</b>
2.1 Introduction.....	4
2.2 Jessen and Howell (1958) .....	4
2.3 Hunt (1962).....	6
2.4 Burger et al. (1981).....	8
2.5 Weingarten et al. (1986) .....	9
2.6 Brown et al. (1993) .....	10
2.7 Hsu et al. (1994).....	12
2.8 Hamouda et al. (1995) .....	13
2.9 Creek et al. (1999) .....	14
2.10 Leiroz and Azevedo (2005) .....	16
2.11 Wax deposition as a whole .....	19
2.11.1 Molecular diffusion of wax.....	19
2.11.2 Shear dispersion of precipitated wax .....	20
2.11.3 Brownian diffusion of precipitated wax .....	20
2.11.4 Gravity settling of precipitated wax.....	21
2.11.5 Sloughing of wax .....	21
<b>ANALYTICAL MEASUREMENTS FOR THE MODEL .....</b>	<b>22</b>
3.1 Mixing the black wax crude oil and diluent .....	22
3.2 FTIR analysis.....	23
3.3 Rheology .....	23
3.4 Composition characterization .....	24
<b>RESULTS OF ANALYTICAL MEASUREMENTS.....</b>	<b>25</b>
4.1 FTIR analysis.....	25
4.1.1 Wax appearance temperature (WAT) .....	25

4.1.2 Estimation of solids .....	27
4.2 Rheology .....	29
4.3 High temperature gas chromatography (HTGC) .....	39
<b>MODELING.....</b>	<b>41</b>
5.1 Introduction to modeling .....	41
5.2 Flow model .....	41
5.3 Temperature model for the pipeline.....	42
5.3.1 Overall heat transfer coefficient.....	43
5.3.2 Inner heat transfer coefficient .....	43
5.3.3 Outside heat transfer coefficient .....	44
5.4 Methods used by DepoWax to predict wax deposition .....	45
5.4.1 Deposition by molecular diffusion.....	45
5.4.2 Deposition of by shear dispersion.....	46
5.5 Input of experimental data into PVTsim and DepoWax.....	46
<b>RESULTS OF MODELING AND CONCLUSIONS .....</b>	<b>48</b>
6.1 Description of the model.....	48
6.2 Case one waxy oil and diluent mixture.....	48
6.3 Discussion of waxy oil and diluent mixture .....	54
6.4 Case two waxy oil and light crude mixture .....	54
6.5 Discussion of light crude and waxy oil mixture .....	59
6.6 Conclusions.....	59
<b>APPENDIX: FLASH OUTPUT FROM PVTSIM.....</b>	<b>61</b>
<b>REFERENCES.....</b>	<b>66</b>

## NOMENCLATURE

Symbol	Definition
$A$	Area Available for Wax Deposition
$C_i^b$	Concentration of $i$ in the Bulk
$C_i^w$	Concentration of $i$ at the Wall
$C_p$	Specific Heat
$C_{wall}$	Volume Fraction of Wax Deposited at the Wall
$d$	Inner Diameter of the Pipe
$D_i$	Diffusion Coefficient of $I$
$Dil$	Percent of Diluent Added
$f$	Friction Factor
$g$	Gravitational Constant
$Gr$	Grashof Number
$h_i$	Inside Heat Transfer Coefficient
$h_o$	Outside Heat Transfer Coefficient

$k$	Thermal Conductivity of Pipe Material
$k^*$	Shear Dispersion Constant, Tuning Parameter
$k_f$	Thermal Conductivity of the Fluid
$\dot{m}$	Mass Flow Rate
$MW_i$	Molecular Weight of $i$
$Nu$	Nusselt Number
$Pr$	Prandtl Number
$Re$	Reynolds Number
$r_i$	Inside Radius of Pipe
$r_o$	Outside Radius of Pipe
$r_w$	Wax Radius
$S_{wet}$	Fraction of the Perimeter Wetted by Current Phase
$T_a$	Ambient Temperature
$T_b$	Bulk Temperature
$T_{in}$	Inlet Temperature
$T_s$	Surface Temperature
$T_x$	Temperature at Location $x$



$U$	Overall Heat Transfer Coefficient
$v$	Linear Velocity
$V_{\text{Diff}}$	Volumetric Diffusion of Wax
$V_{\text{Shear}}$	Volumetric Shear Dispersion of Wax
$x$	Location on Pipe
$x_w$	Deposit Thickness
Greek	
$\alpha$	Thickness Correction Factor, Tuning Parameter
$\beta$	Diffusion Tuning Parameter
$\beta_v$	Volumetric Thermal Expansion Coefficient
$\gamma$	Shear Rate
$\delta$	Thickness of Laminar Sub-Layer
$\partial P/\partial L$	Pressure Drop
$\varepsilon$	Roughness of Pipe
$\theta$	Angle From the Horizontal
$\mu$	Viscosity of the Fluid
$\mu_b$	Viscosity of the Fluid in the Bulk

$\mu_w$	Viscosity of the Fluid at the Wall
$\nu$	Kinematic Viscosity
$\rho$	Density
$\rho_i$	Density of Wax Forming Component i
$\rho_{wax}$	Average Density of Wax in the Bulk

## **ACKNOWLEDGEMENTS**

I would like to thank Dr. Milind Deo for his guidance and financial support over the past year while working on this project. Also working with members of Petroleum Research Center has been a great learning experience. I would also like to thank Dr. Rich Roehner for his tutorial on PVTsim, as well as Dr. Magda for his suggestions and also for serving on my supervisory committee.

My family is also due thanks for their support while working on this project. Also all of the other graduate students I met throughout my studies at the University of Utah.

## **CHAPTER 1**

### **INTRODUCTION**

The need for energy is becoming more crucial these days and is causing more companies to drill for oil that has high paraffin concentrations. The paraffin, also referred to as wax, poses a large problem when it forms and deposits in pipelines carrying this oil. The problem is observed in which the ambient temperature is lower than the wax appearance temperature (WAT), the oil cools and wax will form resulting in deposition. The deposition of the wax decreases the amount of oil traveling through the pipeline and also increases pumping costs. This arises from a decrease in diameter for oil flow. Pipe friction also increases due to solids, i.e., asphaltenes, which can deposit into the wax formation.

There are methods to deal with wax deposition in pipelines. One method is to routinely scrape the deposits from the pipe walls. This method is known as 'pigging'. Other methods include adding chemicals to inhibit the formation of wax in the pipeline. There is also introducing hot oil into the system. This will cause the deposit to be dissolved because it gets heated above its WAT. The problem with this method is that once the deposit has been dissolved back into the hot flowing oil the oil will cool back down further down the pipeline and deposition will continue. Mixing a waxy crude oil with another that does not have as high a wax content is also another method to pump the waxy oil to its final destination.

The method employed to deal with wax deposition is based on the cost of the solution. Regular pigging will keep the pipeline clean and free of deposition. Chemical inhibitors are quite expensive and they have not been shown to completely eliminate wax deposition in pipelines. With the use of the chemical inhibitors, eventually the line must be pigged out adding even more to the cost, although pigging intervals could be at larger time spans. Also with the blending of two oils together, eventually the pipeline will need to be pigged using this type of wax management.

The goal of the treatments is to determine how much and how fast the wax deposit will build up. Using a model to predict deposition thickness over a period of time as well as operating conditions of the pipeline can lead to a better maintenance schedule.

Many groups have researched the wax phenomenon deposition. However due to different testing methods and assumptions made there is a discrepancy on exactly how the mechanisms of deposition occur. There is agreement that the primary mechanisms are diffusion and shear dispersion of wax. The diffusion of wax can occur by dissolved wax diffusing to the wall and depositing and also by the diffusion of wax particles, which have formed in the bulk, to the wall and depositing. Shear dispersion results in transport to the pipe wall based on shear by precipitated wax particles. Shearing can also affect the strength of deposit. If the flowing oil exerts a high enough shear on the deposit, it can be pulled from the wall; this is known as sloughing. When some of the wax sloughs off, the remaining wax is harder.

This thesis models pipeline flow of a high paraffin containing crude oil. This oil flows in a pipeline over a distance of approximately 110 miles with large elevation

changes. The model looks at the addition of a light fraction petroleum distillate, referred to as a diluent, and also looks at blending the black wax crude oil with a lighter crude oil.

## **CHAPTER 2**

### **LITERATURE REVIEW OF WAX DEPOSITION**

#### **2.1 Introduction**

Wax can be defined as paraffin deposits that are insoluble in crude oil at the prevailing producing conditions of temperature and pressure [12]. Wax deposition has always posed a production problem in the petroleum industry. The topic has been studied for many years by many different groups of researchers. The aim of the literature review performed in this chapter is to summarize findings on wax deposition that are available in the literature.

Each paper in this chapter is analyzed paying attention to the hypothesis, the methodology employed, observations and the conclusions made.

#### **2.2 Jessen and Howell (1958)**

Plastic coated pipes used on oil fields, to prevent corrosion, were observed to have little or no wax deposition. Jessen and Howell [12] wanted to verify if different types of pipe as well as different flow rates reduced or eliminated deposition.

The apparatus constructed to test their hypothesis consisted of a flow loop with two test-sections each a length of 5' but varying diameters of 3/4" and 2", made either of plastic, steel or coated pipe with steel being the control. Each pipe material used had the two test-sections. Cooling was achieved by submerging the test-sections in a water bath

by circulating water through coils packed in ice. A hot water bath was also used to keep the circulating oil above its cloud point in the reservoir. Two centrifugal pumps were used in order to produce turbulent flow. The oil transported through the flow loop consisted of microcrystalline waxes in kerosene. In order to control the flow rate of the liquid in the flow loop a series of bypasses were used, this also was used to mix the oil in the reservoir. The flow rate was measured by using a differential manometer placed on each of the test-sections. Tests were run for a time period of about 3 hours. Once a test was completed the test-sections were removed and a tight fitting rubber squeegee was pushed down the pipe in order to collect the paraffin deposit. The paraffin deposit was mixed with pentane and centrifuged at 1,500 rpm for 20 minutes; the solids insoluble in pentane were recorded as paraffin.

Some of the observations made were that the plastic and the coated pipes showed lower deposition than the steel pipe. Another observation made was that as the flow rate was increased the amount of paraffin deposition also increased. The deposition reached a maximum when the flow transitioned from laminar to turbulent flow. Once the flow transitioned to the turbulent regime the deposition decreased rapidly; the plastic pipes with Reynolds numbers greater than 4,000 showed no deposition. The researchers proposed two mechanisms for the paraffin deposition both being due to mass transfer. They also observed viscous drag of the particles exceeding the shear stresses of the deposited paraffin, at higher flow rates.

The first mass transfer mechanism is the diffusion of the paraffin to the wall where the deposit will grow. The second was that paraffin crystals have already formed in the flowing system in which particle diffusion to the wall occurs. The deposition in



the plastic pipes was noticed to be 3 times greater at low velocities when the temperature was 1° F higher than the cloud point than when it was when the oil was 15° F below the cloud point. In the steel pipe not much of a difference was noticed. At the lower temperatures the paraffin crystals would increase, but the deposition did not increase. Since the deposition did not increase with decreased temperature the diffusion of paraffin to the walls was proposed to be controlling.

The viscous drag, at higher flow rates, was proposed to actually remove some of the paraffin from the wall, resulting in the decrease of paraffin deposition. The paraffin deposits at the higher flow rates were also noted to be harder than the paraffin deposits at the lower flow rates.

### **2.3 Hunt (1962)**

Laboratory tests, performed by Elton B. Hunt Jr. [10], were completed in order to determine mechanism of paraffin deposition under similar conditions of well tubing in the field. The studies were completed under steady flow conditions. The author noted that cooling was the controlling factor for wax deposition; this conclusion was made due to no deposition of wax occurring under constant temperature conditions.

The experimental setup consisted of a cold spot apparatus as well as paraffin deposition apparatus. The cold spot test consisted of a cold finger with a plate that was soldered on the end of it and submerged in a stirred heated wax-oil slurry contained in a beaker heated by circulating hot water, while the finger was cooled by circulating cool water. The slurry temperature was decreased at a constant rate of 1.2° F/hour for 15.5 hours. Upon completion of the experiment the plates were removed and examined for the amount of deposit, hardness of deposit and the adherence of deposit to the plate.

A flow loop, for deposition studies, was constructed to mimic the gradients under field conditions. Oil was pumped, at a constant rate from a reservoir maintained at 200° F, through a vertical test section up of 23.3', 1/8" pipe. A precooler was used to cool the incoming oil to the desired temperature at the inlet of the test section. A separate recirculation pump mixed the test section fluid. To prevent oxidation of the hot oil a nitrogen blanket and an oxidation inhibitor were used. The flow loop had two different versions consisting of a high and low temperature gradient used. The experiments were run for 21.5 hours to 155 hours. Once a test was completed the test section was drained and dismantled in some cases the test section was cut into 10" lengths. The dismantled test section was then visually examined and weighed to determine the amount of deposit. The oil was evaporated off of the deposit and then weighed to determine the amount of wax deposited. It was noted that no wax was lost during evaporation.

It was observed that inside the test section specks of wax appeared at the pipe wall near the inlet and become a continuous film of increasing thickness towards the top of the test section. As time increased the deposit became a continuous film throughout the test section. From the results of the visual observations it was proposed that deposition was initiated by direct nucleation of wax on or adjacent to the pipe wall and that the deposit grows by the diffusion of wax to the previously deposited wax. Both the low and high temperature gradient tests gave similar results. From the results of the low and high temperature tests it was concluded that the deposition mechanism does not change when decreasing the temperature gradient.

The results of the cold spot test showed that the wax did not adhere to smooth stainless steel but did adhere to sand blasted stainless steel. It was also observed that the

wax did not adhere to smooth plastic coatings but did adhere when the plastic was roughened by sandpaper. Similar results were made in the test sections. This led to the conclusion that the wax does not adhere to the surface but is held in place by the roughness and/or irregularities of the surface.

#### **2.4 Burger et al. (1981)**

Wax deposition was occurring at the southern end of the Trans Alaskan Pipeline (TAPS), even though the flow rate was high, 1.5 million barrels per day. Burger, Perkins and Striegler [4] wanted to investigate the mechanisms of wax deposition and also wanted to determine the expected nature and the thickness of the deposits found in TAPS. To study the deposition an experimental set up was constructed. The setup consisted of 2.9 m long, 6.35 mm and 12.7 mm stainless steel tubes in parallel horizontal and also parallel vertical configurations. Each of the tubes had its own oil and coolant pumps, allowing independent operation of each tube. All of the tubes were operated under totally laminar conditions and were scaled with wall shear stress rather than the Reynolds number. The temperature and heat flux values were kept in the range of TAPS during initial start-up and early flow. Flow tests lasted from 2 to 200 h, in which the oil and the coolant were both pumped at constant rates. At the end of each test, once the oil was removed, the tubes were heated to 50° C and washed with toluene, for the small diameter tubes. The large diameter tubes were cleaned with a scraper. The amount of deposited wax was determined by the acetone precipitation technique mentioned in the paper. Field test experiments were also completed on 2440 m long with diameters of 10, 15 and 20 cm. Six test sites were spaced at 490 m along each of the pipelines. Each test site had

60 cm spool pieces that were removed, at various time intervals during a test, and the wax scraped to determine the weight and the crystal content.

The total deposition was modeled as the sum of three lateral transport mechanisms molecular diffusion of wax, Brownian diffusion and shear dispersion of the wax particles. Gravity settling was studied for both the horizontal and vertically arranged tubes, but showed no significant effect. The researchers mention that shear dispersion might redisperse settled solids, eliminating any gravity settling effect.

The authors concluded that deposition occurs due to the transport of dissolved and precipitated wax crystals under the conditions in which the oil is cooling. Under different conditions the rate-controlling step varies upon conditions being tested. At high temperature and high heat flux conditions molecular diffusion is controlling, while under the conditions of TAPS, lower temperatures and low heat fluxes, shear dispersion is controlling. It was also found that Brownian diffusion is small when compared to the other mechanisms.

## **2.5 Weingarten et al. (1986)**

Burger [4] described the methods of primary wax deposition to be molecular diffusion, mass diffusion, and shear dispersion. Weingarten and Euchner [21] investigated the two mechanisms independently of one another.

In order to measure deposition due to diffusion only a diffusion cell was built. In the cell the oil was kept static while one end of the cell was heated and the other cooled, to create a temperature gradient. The tests lasted for 48 h to 170 h, with each end maintained at constant temperature. At the end of each test the oil was drained, the cell disassembled and the deposit weighed. The amount of wax was determined by using the

same acetone precipitation technique used by Burger [4]. The results of the diffusion tests found the wax fraction to be constant at 0.18.

The shear dispersion mechanism was also investigated. A flow loop consisting of 1/4" stainless steel tube, for oil, inside a 1/2" copper tube, used to control temperature. Pressure drop across the test section was continuously monitored to calculate the volume of the deposit, assuming the deposit is uniform. The temperature of the oil ranged from 37° F to 66° F, heat transfer rates of 6 BTU/h-ft<sup>2</sup> to 1840 BTU/h-ft<sup>2</sup> and shear rates from 12 s<sup>-1</sup> to 4960 s<sup>-1</sup> were used. Oil temperatures below the wax crystallization temperature were preferred so that the deposition due to diffusion could be accurately measured. Low and high shear rate tests were performed. The rate of deposition due to diffusion and shear dispersion were plotted on the same graph in order to compare results. The low shear rate experiments showed the deposition to gradually increase over time. The deposition over time was greater than that only due to diffusion, which confirmed shear dispersion as a mechanism. The high shear rate tests showed a rapid increase in deposition, similar to diffusion, followed by a decrease and finally resulting in a rate of zero deposition. The decrease of wax deposition was attributed to sloughing off of the wax deposit. The flow for the high shear test remained laminar throughout, meaning that the sloughing occurred when the wall shear stress was greater than that of the wax deposit, not due to turbulence.

## **2.6 Brown et al. (1993)**

Deposition of wax under flowing conditions was studied by Brown, Niesen and Erickson [3]. The results of the experimental tests were then put into a computer model to predict deposition rates at the long term.

The experimental setup consisted of 1/4" and 3/8" stainless steel tubing, each 39" long, submerged in a water bath to control the temperature. Continuous measurements of inlet, outlet and wall temperature were recorded, as well as the pressure drop and the flow rate across the test section. Under laminar flow conditions the deposition thickness can be calculated based on the flow rate and pressure drop, assuming a uniform deposit. The calculated deposition was also compared to the actual deposition by collecting the paraffin and weighing it.

Using Burger's [4] equations of molecular diffusion and shear dispersion, the shear dispersion was tested. To test the shear dispersion mechanism tests were completed at varying shear rates, while maintaining a constant inlet and wall temperature, not a zero flux. At the increased shear rate the deposition actually decreased rather than increased linearly as suggested by Burger. A zero heat flux case was also tested because no molecular diffusion would occur, and shear deposition would be unaffected. No deposition occurred under the zero heat flux condition so it was concluded that shear dispersion does not contribute to deposition.

The modeling of the deposition allows for varying the diffusion coefficient in order to fit experimental data; essentially it has become a data fitting parameter. The model also assumes that the rate of paraffin deposition is slow compared to the rate at which the pipeline comes to a new steady state. It is mentioned that although the pressure drop is a primary variable in the model the roughness of the deposit is much more important, but in the model the roughness value is the same as the thickness of the deposit.

## **2.7 Hsu et al. (1994)**

Most studies involving wax deposition consist of circulating the wax containing crude oil under laminar conditions. Hsu, Santamaria, and Brubaker [11] studied deposition under turbulent conditions.

To conduct the deposition studies a flow loop was built. The flow loop consisted of two identical test sections. The test sections were each 5' long and 0.402" inner diameter stainless steel. The first referred to as the 'test tube unit' was used to test for deposition at various operating conditions. The 'reference tube' was maintained above the oil temperature to inhibit deposition and also used to measure pressure drop to compare to the 'test tube unit' in order to calculate the deposition thickness. Temperature was controlled on each test section using a cooling jacket. The volumetric flow rate, fluid density, system pressure, pressure across the test sections and temperature at various locations were all recorded. At the end of the test nitrogen was used to purge the test sections and then the lines were pigged.

Under turbulent conditions it was found that wax deposition decreased. It was also found that turbulent conditions depress the temperature at which the maximum deposition rate occurs, meaning that the actual pipeline could be operated at lower temperature. The decrease in deposition was explained by a sloughing effect. The higher flow rate created higher shear stresses removing some of the deposit from the wall.

At the completion of each test the tubes were pigged out and the deposit analyzed by simulated distillation and melting point. It was found that with an increase in retention time the deposit showed increases in both hardness and carbon number. At lower oil temperatures the deposit formed was found to be softer. When the oil

temperature approached the ambient temperature, i.e., low heat flux, the deposit was softer and more homogeneous.

## **2.8 Hamouda et al. (1995)**

Of all the deposition mechanisms Hamouda and Davidsen [8] wanted to show that deposition by molecular diffusion is dominant.

The experimental setup consisted of a series of heat exchangers, where oil was kept heated in a tank to maintain temperature while being pumped. The primary heat exchanger, which was the test section, was 25 m long and 1/2" diameter pipe made of aluminum inside of 1" diameter stainless steel pipe. Temperature and pressure measurements were made in every loop of the heat exchanger. Deposition was calculated by measuring the pressure drop across predetermined lengths of pipe. Flow rates were also varied 5 to 11 L/min. The oil was also put under a nitrogen blanket to minimize oxidation.

To study the deposition mechanisms the test pipe was divided into three sections 15, 5 and 5 m. In the first section, 15 m, the oil was cooled from 27° C to 18° C. In the second section, 5 m, the temperature was kept at 17° C. This was done to minimize the temperature gradient to eliminate molecular diffusion. In the final section, 5 m, the conditions of the first section were restored.

The deposition increased between 5 and 7.7 L/min, with a maximum deposition rate at 7.05 L/min. The increase in deposition at these flow rates were due to molecular diffusion and/or shear dispersion, where the temperature and concentration gradient are both factors. Above 7.7 L/min the deposition drastically decreased and zero deposition



occurred at 11 L/min. Deposition decreased due to the increase in the shear stress, which results in the removal of deposition from the wall.

In the second section almost no deposition occurred. If an appreciable amount of deposition occurred shear dispersion would have been considered a larger contributing factor. It was concluded that the shear dispersion is small compared to molecular diffusion and is not a major mechanism.

The investigators also found that deposition occurred for shear rates between  $3500 \text{ s}^{-1}$  and  $5500 \text{ s}^{-1}$ , above the maximum shear rate no deposition was detected. To determine the amount of the deposit a 'paraffin adhesion constant' was defined. This was multiplied by the sum of the amounts of deposition due to shear dispersion and molecular diffusion. When the shear rate was above  $5500 \text{ s}^{-1}$  the constant was set to 0 and when the shear rate was below  $3500 \text{ s}^{-1}$  the constant was set equal to 1. The higher shear rate coincides with the higher flow rate at which no deposition was detected.

## **2.9 Creek et al. (1999)**

Experiments to determine the effects of flow rate and temperature difference on deposition rate, as well as the fraction of oil in the deposit, were performed for single-phase flow by Creek et al. [6]. In this case the shear dispersion was considered insignificant based on previous findings [8].

The flow loop was 50 m long, 43.4 mm inner diameter configured as a horizontal 'U'. The entire tube was jacketed to control temperature. At every 5 m along the tube temperature and pressure measurements were taken. Wax deposits were collected from removable spools located at 20 m from the inlet and 5 m from the outlet. Flow rate of the oil and coolant was also measured. Pressure drop, energy balance based on temperature

difference, volume changes in the test section, ultrasonic transit time and direct measurement were the different methods used to determine deposit thickness in the study. The fraction of oil in the deposit was determined by high temperature gas chromatography. Modeling software, from Multiphase Solutions Inc. by Brown [3], was also used alongside the experiments.

The temperature difference between the oil and wall was the first study performed. Both laminar and turbulent flow was tested for this case. Both show a linear increase in deposition with the laminar case having thicker deposits. The deposits found in the test section under the laminar case were found to be much softer than for the turbulent case. Another note about deposit hardness was that the larger the difference in temperature between the oil and the wall, the softer the deposit. The modeling software followed the same trend as the experimental results and gave near what was measured for deposition [3].

Another test that was performed was to keep a constant temperature difference between the pipe wall and flowing oil of  $8.3^{\circ}\text{C}$  while decreasing the inlet temperature of the oil to as much as  $25^{\circ}\text{C}$  below the wax appearance temperature (WAT). These tests were performed under laminar conditions. It was also found that no deposition was observed when there was no temperature difference. The modeling software for this case also gave the same trend but there was more scatter among all the methods used to calculate deposit thickness [3].

Using the same temperature difference of  $8.3^{\circ}\text{C}$  between the flowing oil and the wall, the effect of varying flow rate was also tested. As the flow rate was increased it was found that the deposit thickness decreased. This was true for both turbulent and

laminar flow. The result from the turbulent tests showed that the wax content of the solid was between 60 and 80%. Sloughing was also mentioned as the reason why the deposit decreased in thickness over time. The modeling software showed the inverse of what was measured for increasing flow rate. It showed an increase in deposit thickness and then a decrease [3].

During the measurements of the deposition thickness the energy balance method was found to fit the data for deposition thickness more accurately for laminar flow conditions. The pressure drop method for calculating deposit thickness proved to be more accurate for turbulent flow conditions.

### **2.10 Leiroz and Azevedo (2005)**

Leiroz and Azevedo [13] noticed that in models predicting wax deposition constants were adjusted in order to fit the predictions of the model for the actual data collected, either from the field or laboratory. This was good for a specific scenario, but not the importance of individual mechanisms. The study used experiments and numerical analysis to study diffusion-based mechanisms.

The study employed two deposition tests, both using a model oil. The first test for deposition was under stagnant conditions. The model oil for the stagnant tests consisted of a 10% by volume solution of paraffin. The paraffin solution consisted of carbon numbers of C21 to C38. The paraffin solution was then dissolved in n-paraffin. The WAT for the model oil was determined to be 27° C the properties of the oil were also known. The experimental set up for the stagnant tests consisted of a deposition cell. The cell had dimensions of 10 x 30 x 0.5 mm. The 0.5 mm was the area available for deposition this was made by “sandwiching” two pieces of glass together, held in place by

copper fins. The fins had thermocouples attached to each to record the temperature. The oil was pumped into the cell, and temperature in the cell was maintained above the WAT. During the test one side of the cell remained hot and the other side was cooled. This allowed for the deposition to be recorded and digitized.

The experiments under laminar flow conditions used a model oil with a WAT of 36° C and consisted of a rectangular test section with dimensions of 3 x 10 x 300 mm. The walls of the test section were made of 2 mm glass plates and the top and bottom of the test section was made of copper, which was soldered to hollow copper blocks. The copper blocks had water pumped through them, in order to control and maintain temperature. Temperature was monitored by thermocouples attached to the copper walls. The temperature of the oil was controlled upstream with a coil-tube heat exchanger. An electric heater heated a smaller tank downstream, previous to the test section, in order to avoid deposition before entering the test section. To study the deposition the oil was allowed to flow above the WAT until a steady state condition was achieved, after steady state was achieved cold water was circulated through the copper blocks to cool the test section. To visualize the whole length of the test section, the flow rate was set and a camera was set at a specified location once the cooling began the camera began to record the test section. After deposition was achieved, the copper blocks were heated to remove the deposition and the test was repeated under the same conditions with the camera moved further down the test section. This was done until the entire test section was recorded.

Simulations of the experiments were also completed. The model for the stagnant experiment consisted of the following assumptions: one-dimensional heat and mass

transfer, constant properties and saturated liquid at the solid fluid interface. The model for the laminar flow system assumed one-dimensional flow, with velocity varying in the axial direction due to the deposition of wax. The flow also employed the use of a friction factor. Heat losses were also calculated for each of the walls. Burger's [4] molecular diffusion model accounted for the growth of the deposited layer.

When the results were modeled for the stagnant condition it was concluded that the model for molecular diffusion under predict the actual amount of deposition. This led the authors to believe that the other mechanisms do play a role, although heat losses in the walls of the deposition cell were not considered.

From the experimental results of the laminar flow condition it was observed that the deposition on the top of the test section was equal to the deposition on the bottom of the test section. The symmetry of the deposition visually showed that gravity settling was not a relevant mechanism of deposition. The authors also found that in their experiments within the first 10 minutes of testing the deposition was about 50% of the final steady state deposition. Another observation made by the authors was that with increase of axial length, deposition increases, while the model predicts a decrease. The only agreement of data came from the steady state condition, in which both the experimental results and the model show an increase in deposition. The conclusion of the study shows that the models under predict the actual deposition when only molecular diffusion is considered. This implies that other mechanisms do in fact play a role in deposition.

## **2.11 Wax deposition as a whole**

In this area many groups have researched and proposed ideas of the mechanisms of deposition. Many experiments have been carried out to study this phenomenon. The experiments carried out either were used to focus on one type of deposition mechanism or to study it as a whole. The purpose for carrying out this research is to predict the amount of wax deposited as well as the properties of the deposit. This is very important in order to mitigate wax deposition. It has been found that changing certain operating parameters can help to minimize the deposition of wax in a pipeline. It is also useful to know, if deposition cannot be prevented, when treatment of the pipeline may become necessary. The treatments can include chemical inhibitors or mechanical methods (pigging). From the literature reviewed previously the mechanisms of deposition were found to be:

1. Molecular diffusion of dissolved wax
2. Shear dispersion of precipitated wax
3. Brownian diffusion of precipitated wax
4. Gravity settling of precipitated wax
5. Sloughing of wax

### **2.11.1 Molecular diffusion of wax**

Molecular diffusion of wax is based on a concentration difference. It is also affected by temperature gradients within the flowing pipeline. This problem can be seen in pipelines in which the oil is flowing below the Wax Appearance Temperature (WAT) over long distances. With oil being a mixture of many different hydrocarbons concentration gradients will develop rapidly once the oil temperature falls below the WAT, due to each component having its own temperature dependence on solubility in the

solution. This mechanism of deposition has been found to be very important in deposition studies and has also been confirmed by many different groups [3, 4, 6, 8, 13]. Molecular diffusion of wax will be investigated later in this thesis using the DepoWax module found in PVTsim by Calsep International Consultants.

### **2.11.2 Shear dispersion of precipitated wax**

Shear dispersion occurs when the wax particles move across fluid streamlines due to differences in shear imparted by other flowing particles. The particles in solution rotate as they flow, and due to the viscosity of the fluid the rotating particles will impart a shear force on nearby particles. In a high presence of particles the interactions between them will increase and the lateral transport of wax particles will occur across the streamlines toward the wall and deposit. Shear dispersion is considered to be one of the major mechanisms in wax deposition and appears to play a bigger role at lower temperatures as well as lower heat fluxes [3, 4, 6, 21]. Shear dispersion is the second mechanism considered in the DepoWax module and will be used in the modeling of wax deposition in this thesis.

### **2.11.3 Brownian diffusion of precipitated wax**

Brownian diffusion of precipitated wax is based on random movements of the precipitated particles. This is also affected by concentration of wax particles in solution. Typically the particles in solution will have no net displacement. In the case of high concentration of suspended wax particles in a flowing system, collisions will increase and the particles will move towards the wall where there is a lower concentration. Brownian diffusion is not considered to play a pivotal role in wax deposition because it is small

compared to other mechanisms of wax deposition. As mentioned by Burger [4], Brownian diffusion was prominently mentioned in the USSR literature. In this thesis Brownian diffusion is not considered.

#### **2.11.4 Gravity settling of precipitated wax**

Gravity settling occurs when a heavier particle settles due to the force of the Earth's gravity. Wax particles are denser than the surrounding fluid and will begin to settle out under stagnant conditions. Under flowing conditions, especially under turbulent conditions, as the particles settle out the flow can cause settled wax particles to return to the bulk. The shear dispersion can also remove the wax particles that have settled out due to gravity. Due to the previously mentioned reasons, gravity settling of wax particles is not considered to play a large role in wax deposition.

#### **2.11.5 Sloughing of wax**

In sloughing of wax the wax layer actually decreases in thickness [3, 8, 11, 12]. This arises from the shear stress felt by the deposit on the wall. When the shear stress increases beyond the yield stress of the deposit, the deposit is sloughed off. This mechanism is not studied in this thesis but does play a vital role for the restart of plugged pipelines.



## **CHAPTER 3**

### **ANALYTICAL MEASUREMENTS FOR THE MODEL**

The DepoWax module in PVTsim allows the fluids to be characterized based on analytical measurements. The use of the analytical measurements in the modeling software allows for a more accurate simulation.

The analytical measurements were performed on the black wax crude oil, as well as other samples of the black wax crude oil with a diluent added at varying weight percentages. The measurements that were performed were wax appearance temperature and estimation of solids percentage, viscosity and compositional characterization.

#### **3.1 Mixing the black wax crude oil and diluent**

The crude oil the oil had to be heated, since it was solid at room temperature. The crude oil was heated in a beaker on a hot plate with a stirrer inside until it melted and became possible to transfer a known amount. The diluent was liquid at room temperature, made up of mostly light end carbons. The mixing was done based on weight percent. First the crude oil, once melted, then it was transferred to sample bottle using a Pasteur pipette that was placed on a digital scale that was zeroed. The amount of oil and diluent mixed in the sample bottle all depended on the weight percent of the mixture being tested. The samples prepared were a 10%, 30% and 50% by weight

--

diluent mixture. Once these were mixed the sample bottles were capped, to eliminate evaporation of diluent, and labeled in order to perform analytical tests on them later.

### **3.2 FTIR analysis**

WAT and an estimate of the amount of solid wax in the sample at different temperatures were determined using an FTIR technique developed by Roehner [18].

Using this method, the IR spectra of the crude oil ( $4000\text{ cm}^{-1}$  to  $600\text{ cm}^{-1}$ ) were obtained for temperature ranges varying from sample to sample. The temperature ranged from  $60\text{ }^{\circ}\text{C}$  to  $3.0\text{ }^{\circ}\text{C}$ . IR absorbance of the sample was measured in a temperature controlled liquid cell that was held between clear and polished NaCl windows in a Perkin Elmer FTIR Spectrometer. Sixteen scans were performed at each of the temperatures used.

The area of interest of the samples was the peak area found between the range  $735\text{--}715\text{ cm}^{-1}$ , attributed to the rocking vibrations of long chain methylene groups. The software included with the spectrometer calculated the peak area. A plot of the peak area versus temperature was created in a spreadsheet where the WAT was determined and the solids weight percentage was estimated.

### **3.3 Rheology**

Below the WAT the crude oil displays time-dependent, non-Newtonian shear thinning behavior, as the shear stress increases the viscosity of the fluid decreases. The viscosity measurements were performed on the black wax crude oil as well as the 10%, 30% and 50% by weight diluent mixtures.

Viscosity was measured using a Brookfield DV-II+ cone and plate viscometer. A sample size of 1.0 mL was used for each of the viscosities measured. Once the sample was placed, the plate was locked in place creating a closed system for the sample. Once locked in place the plate was then heated above the WAT to remove any memory from the sample. Viscosities were measured at varying temperatures by setting a predetermined temperature and allowing the sample to come to equilibrium at that temperature. Using different shear rates, at the maintained temperature, viscosity was measured to get a time-independent value of viscosity. The viscosity collected was a function of temperature as well as shear rate.

### **3.4 Composition characterization**

To obtain a carbon number distribution of the black wax crude oil, high-temperature gas chromatography (HTGC) was performed on it as well as the diluent. The carbon number distribution plays an important role when characterizing the fluids in the DepoWax module.

The procedure used for this was an HTGC simulated distillation (HTGC-SimD) [7] based on ASTM D-5307 [19]. This procedure results in the total weight percent of the single carbon number (SCN), along with the weight percentages of n-alkane and non-n-alkanes of each SCN. The modified procedure gives the weight percentages of SCNs up to SCN 80. The n-alkane corresponds to the paraffin content, to get wax fraction the n-alkane weight percent is divided by the SCN. These tests were completed at the Energy and Geoscience Institute at the University of Utah.

## **CHAPTER 4**

### **RESULTS OF ANALYTICAL MEASUREMENTS**

The results from the analytical measurements performed, as described in the previous chapter, are presented here. The results from the analytical measurements play a large role in characterizing the fluids in the DepoWax database. Use of the analytical measurements allows for the model to more accurately represent the flow in the pipeline.

#### **4.1 FTIR analysis**

##### **4.1.1 Wax appearance temperature (WAT)**

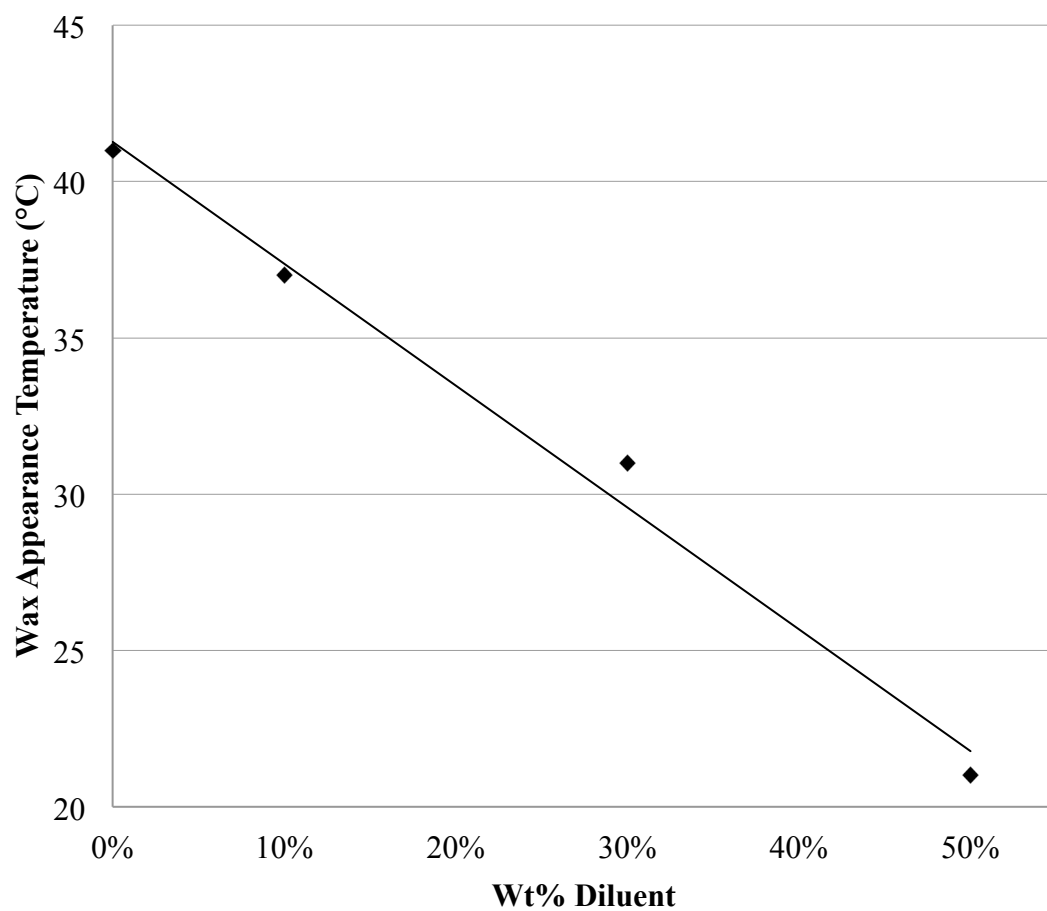
FTIR analysis was performed on the black wax crude oil and the 10%, 30% and 50% by weight diluent and crude oil mixtures. The WAT decreased with increasing amounts of diluent. The WAT showed a linear trend for the case of no addition of diluents to adding 50% diluent by weight and is given by the following equation:

$$\text{WAT} = -38.98 * D + 41.27 \quad (4.1)$$

where D represents the percent of diluent added. Values of WAT for each of the different amounts of diluent are shown in Table 4.1. Also shown in Figure 4.1 is the linear trend that the WAT followed for different dilutions tested.

**Table 4.1** WAT from FTIR analysis.

<b>Weight % Diluent</b>	<b>Wax Appearance Temperature (°C)</b>
0	41
10	37
30	31
50	21

**Figure 4.1** WAT for different amounts of diluent added.

#### 4.1.2 Estimation of solids

Also with the WAT an estimation of solids percentage was completed on the same samples. Each of the samples shows a similar behavior that was expected as the temperature continues to decrease the amount of solids increase. Eventually the solids amount levels off showing that all of the solids have precipitated out of solution. Similar to the WAT, when the amount of diluent was increased the amount of solids in the sample decreased. The weight percent solids vs. temperature graphs are shown for each of the samples in Figure 4.2 to Figure 4.5.

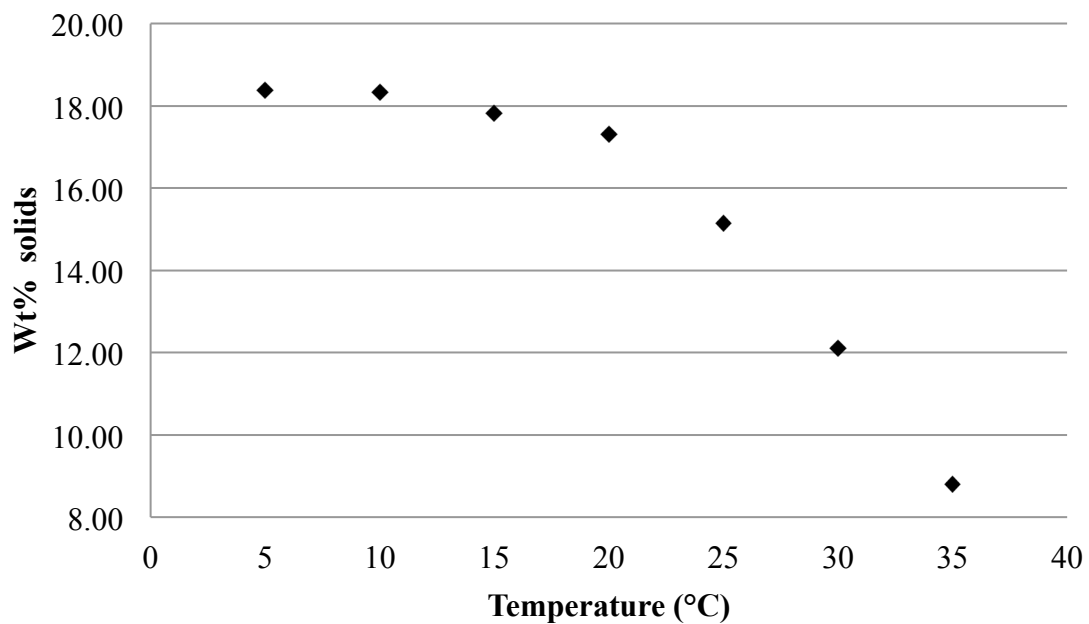


**Figure 4.2** Weight percent solids for the black wax crude oil.

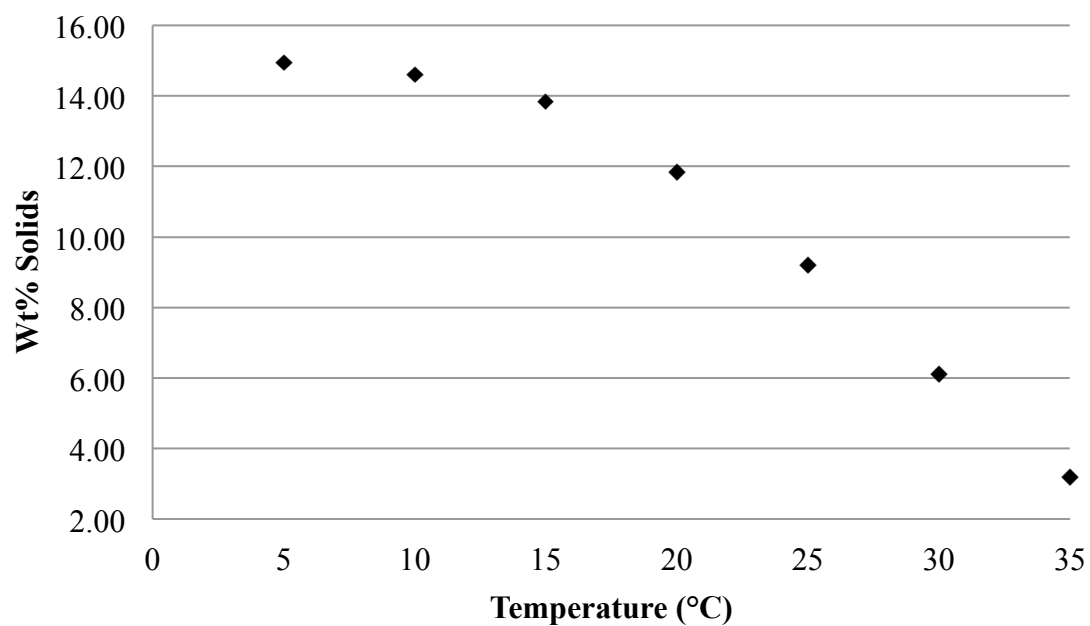


**Figure 4.3** Weight percent solids for the 10% by weight diluent mixture.

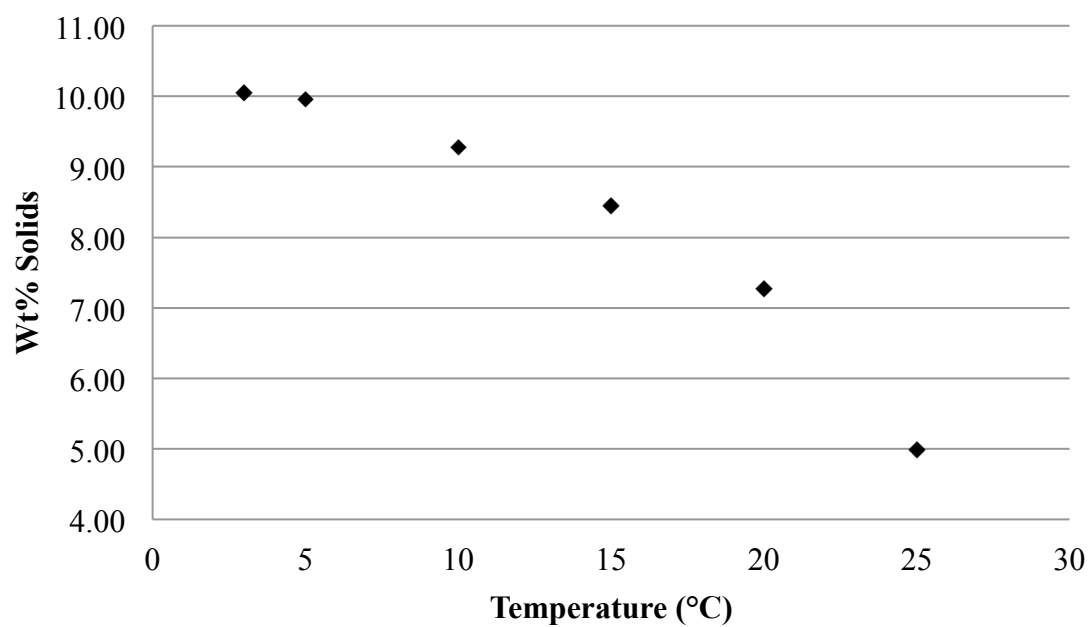


**Figure 4.4** Weight percent solids for the 30% by weight diluent mixture.

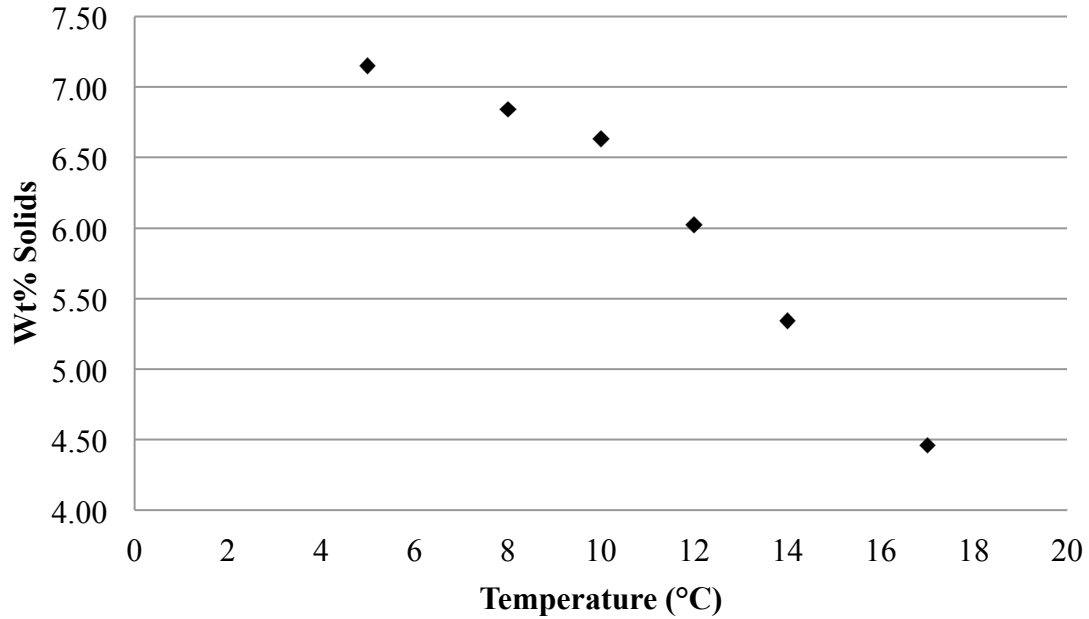


**Figure 4.5** Weight percent solids for the 50% by weight diluent mixture.

## 4.2 Rheology

The viscosity of the waxy crude oil increases rapidly as the temperature decreases and then becomes a solid once it has cooled below its WAT. With the oil turning to a solid once it continues to cool below its WAT the pipeline the oil is flowing in can become plugged. With the addition of the diluent to the waxy sample the viscosities were affectively decreased. With increasing amounts of diluent added viscosities were decreased from the original black wax. The values of the viscosity and strain rate are both used in the DepoWax module. Viscosities vs. strain rate at varying temperatures are shown in Figure 4.6 to Figure 4.9. Accompanying the previously mentioned figures are Table 4.2 to Table 4.5 showing the strain rate, shear stress and temperature of each of the samples.



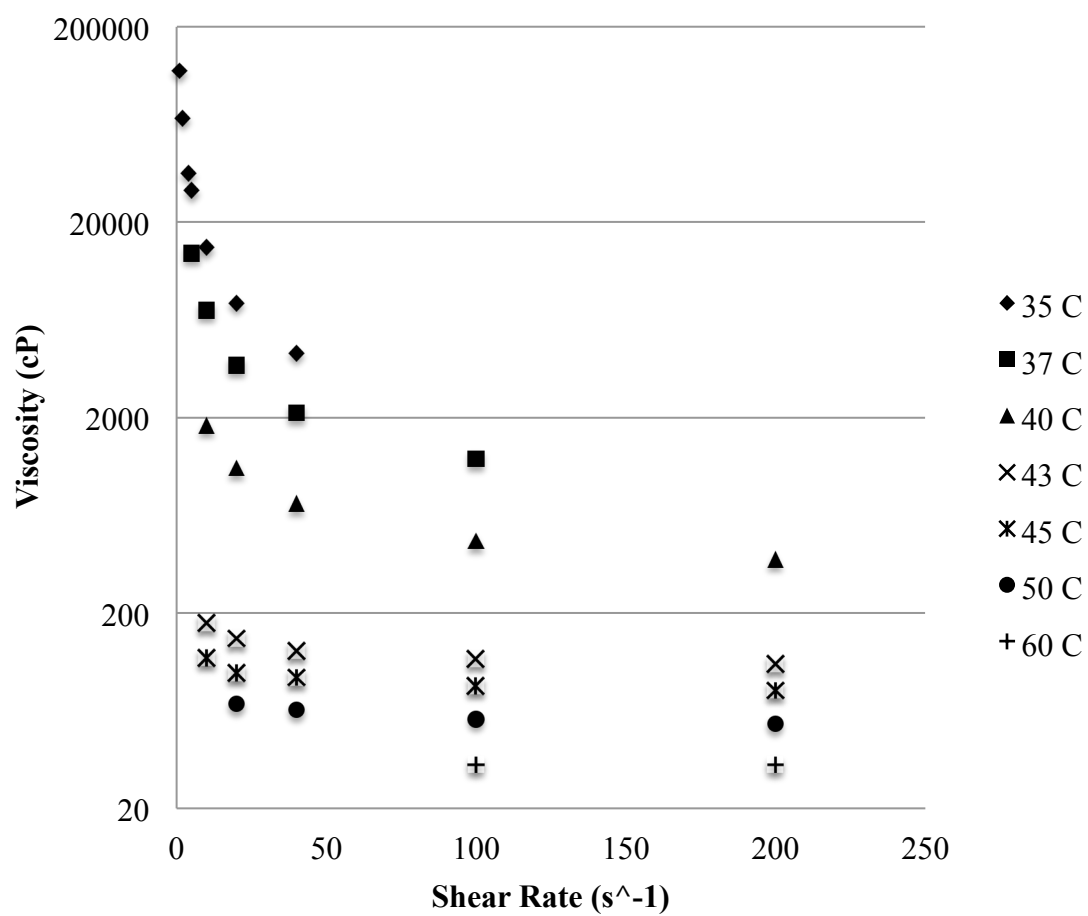


**Figure 4.6** Viscosity of the waxy crude oil at varying temperatures and shear rates.

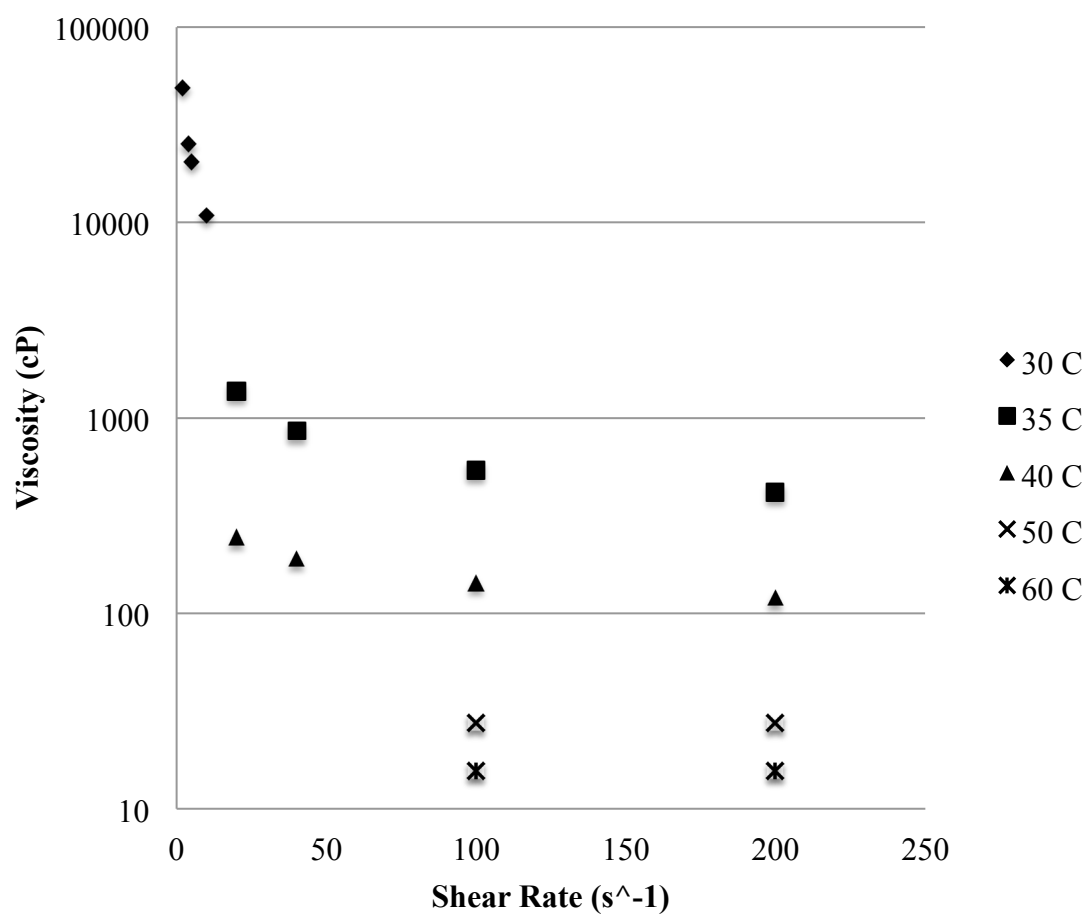


**Figure 4.7** Viscosity of the 10% by weight diluent mixture at varying temperatures and shear rates.

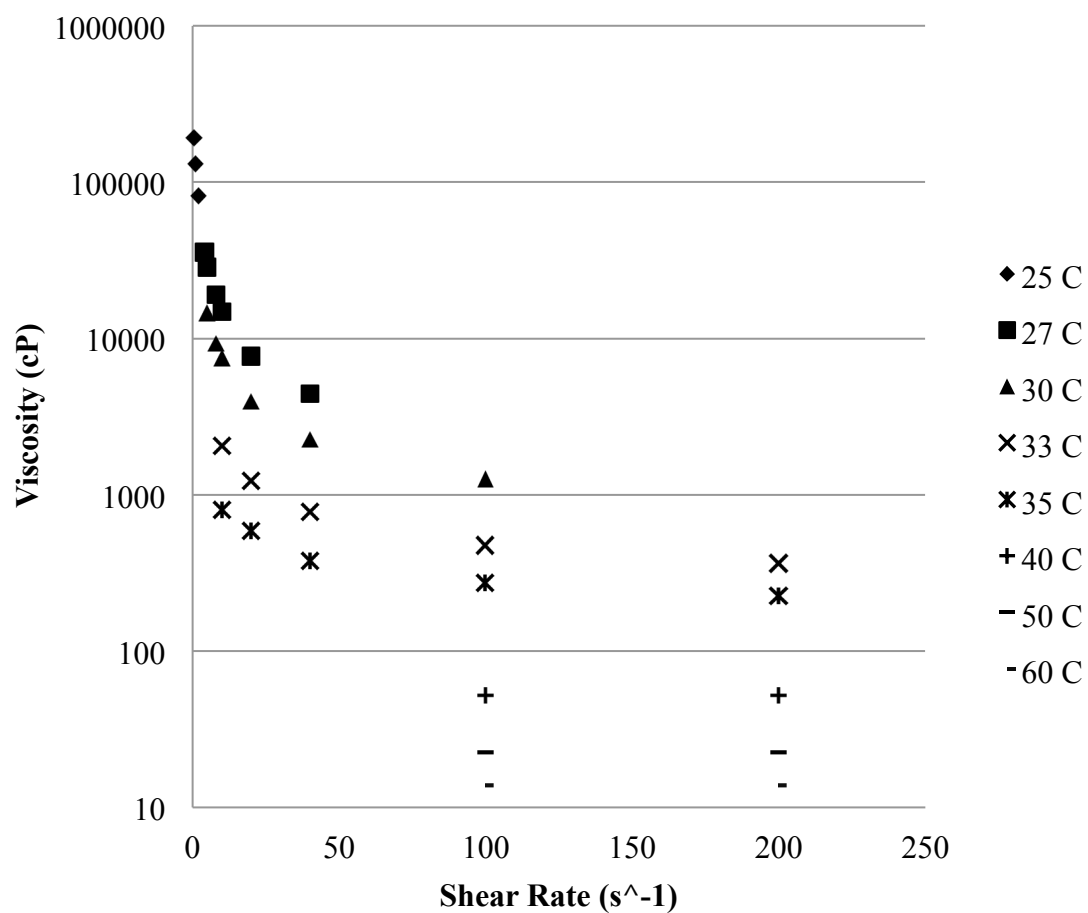


**Figure 4.8** Viscosity of the 30% by weight diluent mixture at varying temperatures and shear rates.

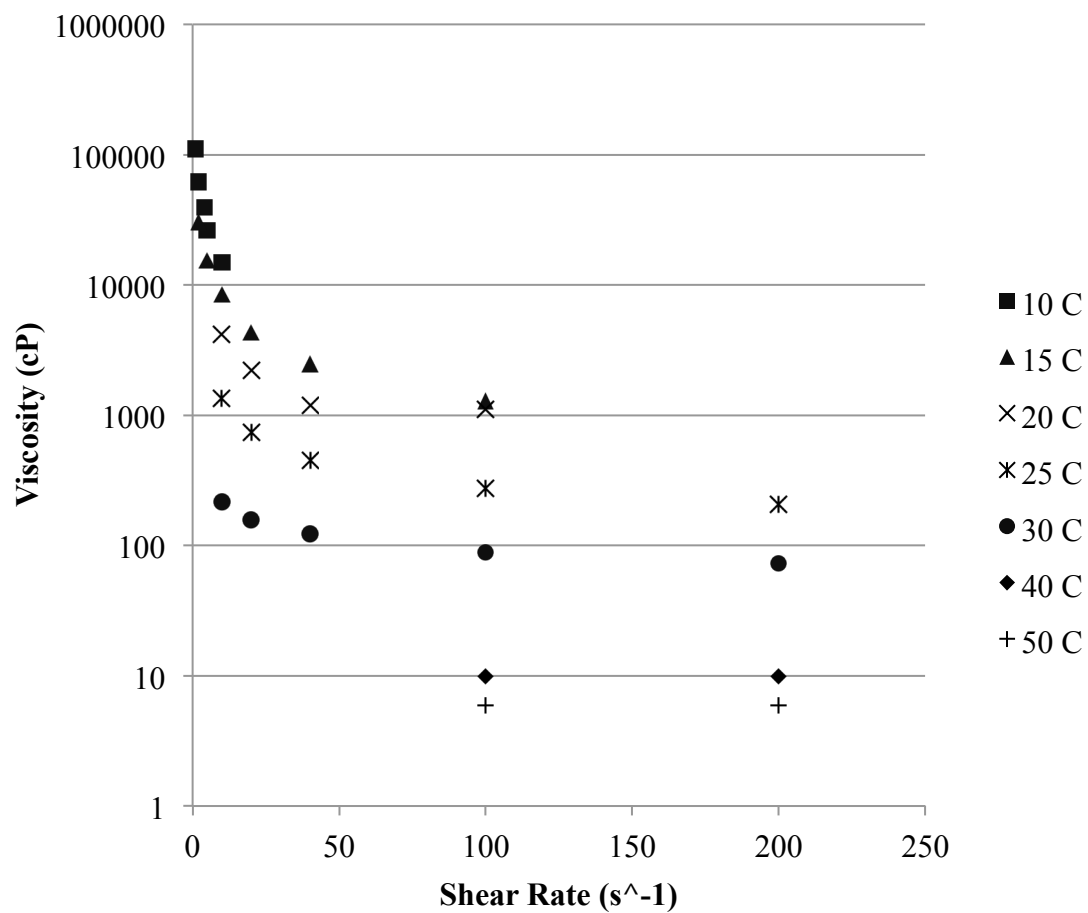


**Figure 4.9** Viscosity of the 50% by weight diluent mixture at varying temperatures and shear rates.

**Table 4.2** Shear stress and strain rate at varying temperatures for the waxy crude oil.

Temperature (°C)	Shear Stress (Pa)	Strain Rate (s <sup>-1</sup> )
60	66.8	200
60	33.4	100
50	108.1	200
50	57	200
50	25	40
50	13.8	20
45	161.2	200
45	84.5	100
45	37.4	40
45	19.7	20
45	11.8	10
43	218.2	200
43	116	100
43	51.1	40
43	29.5	20
43	17.7	10
40	753	200
40	469.9	100
40	291	40
40	222.2	20
40	182.8	10
37	1230	100
37	849.3	40
37	743.1	20
37	709.7	10
37	692	5
35	1708	40
35	1537	20
35	1486	10
35	1449	5
35	1421	4
35	1366	2
35	1187	1

**Table 4.3** Shear stress and strain rate at varying temperatures for the 10% by weight diluent mixture.

Temperature (°C)	Shear Stress (Pa)	Strain Rate (s <sup>-1</sup> )
60	31.5	200
60	15.7	100
50	27.5	200
50	13.8	100
40	241.8	200
40	143.5	100
40	76.7	40
40	49.2	20
35	815.9	200
35	536.7	100
35	344.1	40
35	277.2	20
30	1095	10
30	1018	5
30	998	4
30	985	2
30	924	1

**Table 4.4** Shear stress and strain rate at varying temperatures for the 30% by weight diluent mixture.

Temperature (°C)	Shear Stress (Pa)	Strain Rate (s <sup>-1</sup> )
60	27.5	200
60	13.8	100
50	45.2	200
50	22.6	100
40	100.3	200
40	52.1	100
35	450.2	200
35	273.3	100
35	153.3	40
35	118	20
35	80.6	10
33	723.5	200
33	475.8	100
33	308.7	40
33	245.8	20
33	204.5	10
30	1260	100
30	906.3	40
30	792.3	20
30	759	10
30	723.5	5
30	719.6	4
30	613.4	2
30	442.4	1
27	1757	40
27	1549	20
27	1474	10
27	1437	5
27	1427	4
27	1013	2
27	812	1
25	1633	2
25	1303	1

**Table 4. 5** Shear stress and strain rate at varying temperatures for the 50% by weight diluent mixture.

Temperature (°C)	Shear Stress (Pa)	Strain Rate (s <sup>-1</sup> )
50	11.8	200
50	5.9	100
40	17.7	200
40	9.83	100
30	145.5	200
30	88.5	100
30	49.2	40
30	31.5	20
30	21.6	10
25	414.9	200
25	273.3	100
25	180.9	40
25	149.4	20
25	133.7	10
20	713.7	100
20	479.7	40
20	436.5	20
20	420.7	10
15	1299	100
15	1010	40
15	855.2	20
15	841.4	10
15	772.6	5
15	640.9	2
10	1480	10
10	1311	5
10	1280	4
10	1234	2
10	1101	1



### 4.3 High temperature gas chromatography (HTGC)

Characterization of the oil by HTGC was also used to characterize the fluid in the DepoWax module. The waxy crude oil had carbon numbers as high as C81. The distribution can be seen in Figure 4.10. The diluent used also had the HTGC procedure performed on it and consisted of carbon numbers below 10; this distribution is shown in Figure 4.11. The light crude oil used in the modeling process was previously used [14] in another study. The carbon number data, from the previous study, were used to characterize the light crude oil and can be seen in Figure 4.12.

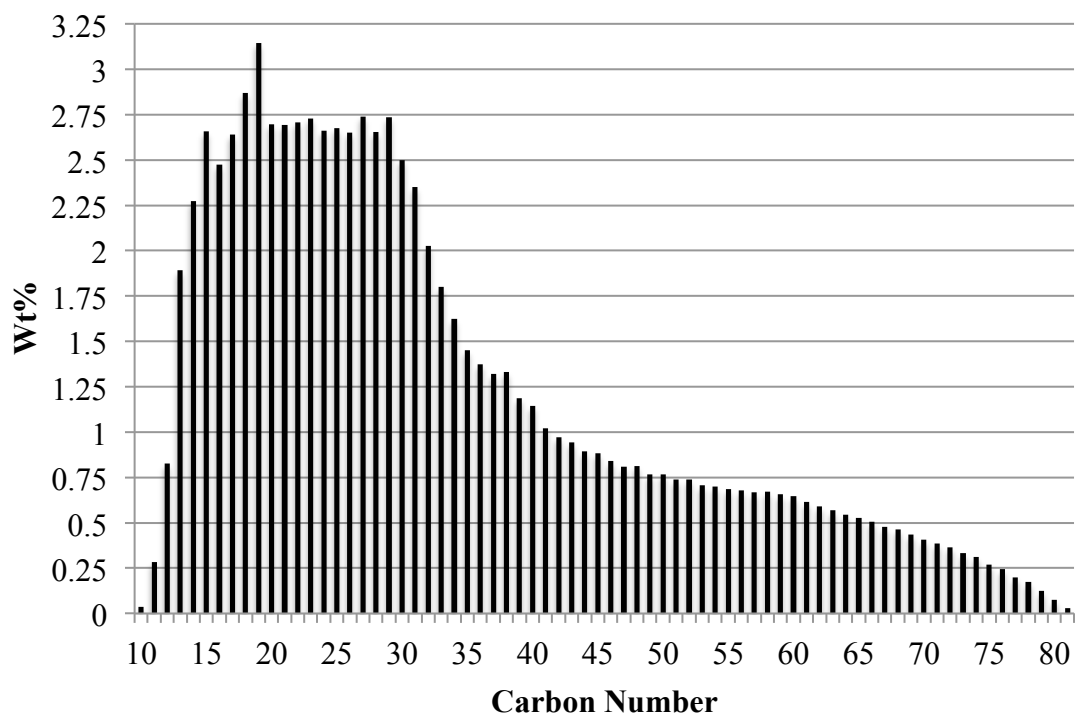


**Figure 4.10** Carbon number distribution of the waxy crude oil.

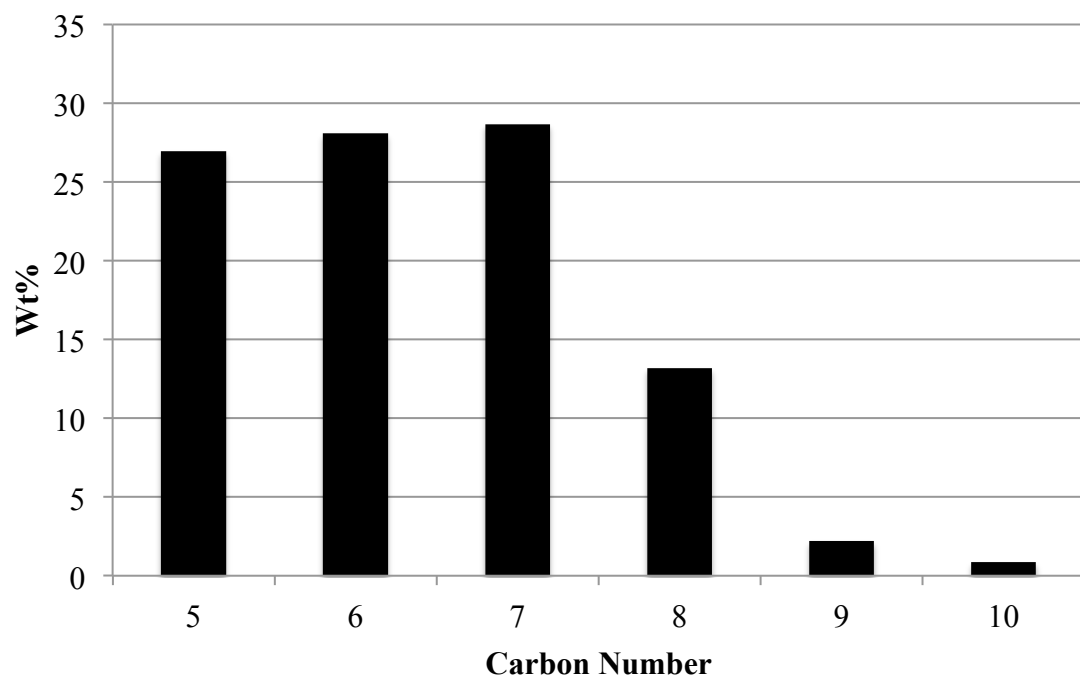


**Figure 4.11** Carbon number distribution of the diluent.

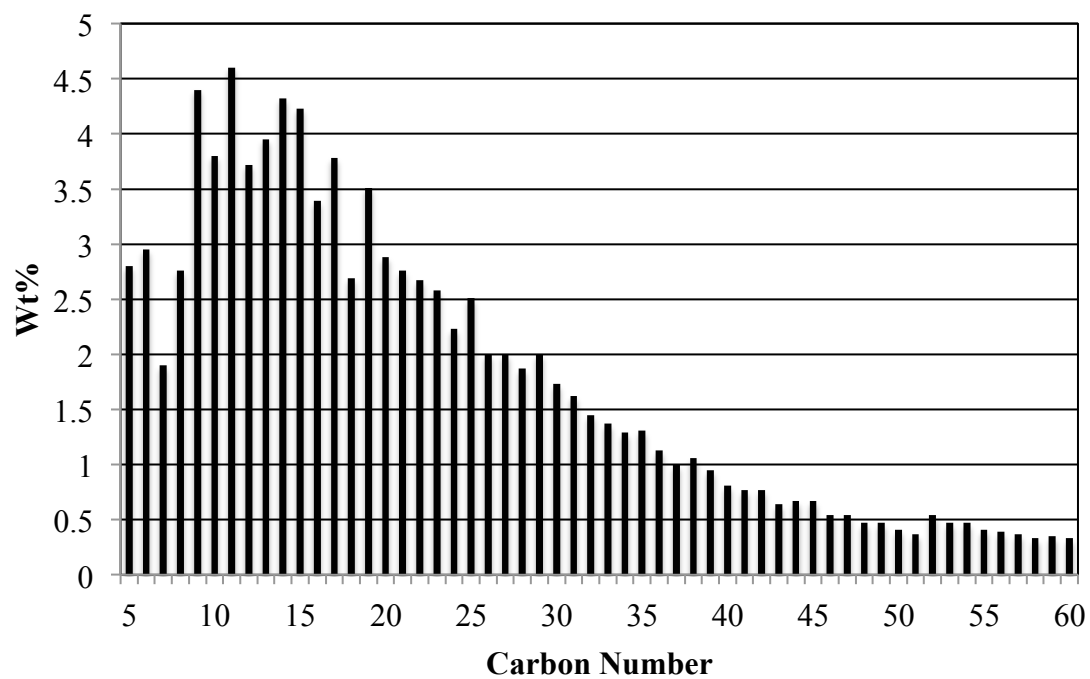


**Figure 4.12** Carbon number distribution of the light crude oil.

## **CHAPTER 5**

### **MODELING**

#### **5.1 Introduction to modeling**

The modeling conducted in this thesis was performed using a commercially available simulation package. The program, PVTsim by Calsep International Consultants, contains a module called DepoWax. This module makes it possible to predict wax deposition in crude oil carrying pipelines. As described in the previous chapters the modeling of the flow becomes more reliable if analytical measurements are made in the lab and the oil that is being modeled is characterized. Without the characterization of the oil being used PVTsim can calculate properties of the oil based on thermodynamic calculations. However these calculations may not be the same as what was measured in the lab. The following section describes the methods the DepoWax module employs to model the deposition of wax in the pipeline [16, 17].

#### **5.2 Flow model**

In DepoWax there are two flow models used one for single-phase flow and another for two-phase flow. Single-phase flow was only considered in this thesis. The flow model is given by

$$\left(\frac{\partial P}{\partial L}\right)_{Total} = \rho g \left( \sin \theta + \frac{fv^2}{2d} \right) \quad (5.1)$$

where  $\rho$  is the density fluid,  $g$  is the acceleration due to gravity,  $\theta$  is the angle of the pipeline from the horizontal,  $v$  is the linear velocity and  $d$  is the inner diameter of the pipeline. The term  $f$  is the friction factor and is a function of the roughness of the pipe,  $\varepsilon$ , inner diameter and the Reynolds number. The friction factor can be calculated from the following expression

$$f = 5.5 \times 10^{-3} \left( 1 + \left( 2 \times 10^4 \frac{\varepsilon}{d} + \frac{10^6}{\text{Re}} \right)^{1/3} \right) \quad (5.2)$$

The Reynolds number is the ratio of inertial to viscous forces.

$$\text{Re} = \frac{\rho v d}{\mu} \quad (5.3)$$

### 5.3 Temperature model for the pipeline

The rate of heat transfer from the oil through the pipe wall and to the environment or vice versa depending on the time of year or location of the pipeline is a very important factor in the transport of the wax containing oil. As the temperature begins to drop the amount of wax appearing in solution will increase. An energy balance is used in which the pipeline is divided into sections and a temperature can be calculated at a position  $x$ .

$$T_x = T_a + (T_{in} - T_a) \exp \left( \frac{-\pi d U}{C_p \dot{m}} x \right) \quad (5.4)$$

From the above equation a temperature profile can be calculated with knowledge of the mass flow rate  $\dot{m}$ , the specific heat  $C_p$ , pipeline diameter  $d$  and the overall heat transfer coefficient  $U$ .  $T_a$  represents the ambient temperature and  $T_{in}$  is in temperature of the inlet.

### 5.3.1 Overall heat transfer coefficient

The overall heat transfer coefficient takes into account the inner,  $h_i$ , and outer heat transfer,  $h_o$ , coefficients as well as the thermal conductivity,  $k$ , of the pipeline and is calculated by

$$U = \frac{1}{r_i} \left( \frac{1}{r_i h_i} + \sum_{i=1}^n \frac{\ln \frac{r_i}{r_{i-1}}}{k_{i-1,1}} + \frac{1}{r_o h_o} \right)^{-1} \quad (5.5)$$

in this equation  $r_i$  is the inner radius and  $r_o$  the outer radius. The term  $k_{i-1,1}$  represents the thermal conductivity of the wax between the two radii  $r_{i-1}$  and  $r_i$ . As the deposition increases the program uses an additional layer wax radius,  $r_w$ , which is a function of deposit wax thickness,  $x_w$ , and the inner radius of the pipe and is given by

$$r_w = r_{in} - x_w \quad (5.6)$$

### 5.3.2 Inner heat transfer coefficient

The inner heat transfer coefficient depends on the flow regime laminar, transitional or turbulent and is based on the Nusselt number,

$$Nu = \frac{h_i d}{k_f} \quad (5.7)$$

where  $k_f$  represents the thermal conductivity of the fluid. The Nusselt number can be calculated from correlations to the dimensionless Reynolds and Prandtl numbers,

$$Pr = \frac{c_p \mu}{k_f} \quad (5.8)$$

The correlations are also based on what flow regime the fluid is in. DepoWax uses the Sieder-Tate correlation as the default selection for the calculation of the inner heat transfer coefficient. This correlation was used for this thesis. When the Reynolds number is greater than 10,000 the Nusselt number is given by

$$Nu = 0.027Re^{0.8}Pr^{1/3} \left( \frac{\mu_b}{\mu_w} \right)^{0.25} \quad (5.9)$$

where  $\mu_b$  is the viscosity of the fluid in the bulk and  $\mu_w$  is the viscosity of the fluid at the wall. When the Reynolds number falls between 2,300 and 10,000 the Nusselt number can be calculated by

$$Nu = 0.027Re^{0.8}Pr^{1/3} \left( 1 - \frac{6 \times 10^5}{Re^{1.8}} \right) \left( \frac{\mu_b}{\mu_w} \right)^{0.25} \quad (5.10)$$

When the flow is laminar, and the Reynolds number is less than 2,300 the Nusselt number is given by

$$Nu = \max \left( 0.184(GrPr)^{1/3}, 3.66 \right) \quad (5.11)$$

DepoWax uses the maximum number from Equation 5.11, typically the value of 3.66 is used for the laminar flow regime. Gr is the Grashof number and is given by

$$Gr = \frac{g\beta_v(T_s - T_b)d^3}{\nu^2} \quad (5.12)$$

in the above equation  $g$  is gravity,  $\beta$  is the volumetric thermal expansion coefficient, the two temperatures  $T_s$  and  $T_b$  are at the surface and in the bulk and  $\nu$  is the kinematic viscosity of the fluid.

### 5.3.3 Outside heat transfer coefficient

The outer heat transfer coefficient is a specified value that remains constant for a given section of pipe. Heat transfer coefficients can be specified for free or forced convection in air or water. Free convection for air was used in this thesis and was specified at a value of 4000 mW/m<sup>2</sup>\*°C.

## 5.4 Methods used by DepoWax to predict wax deposition

### 5.4.1 Deposition by molecular diffusion

The DepoWax module can consider wax deposition from the oil phase or the gas phase. The gas phase is not applicable to this thesis. Only two of the mechanisms are considered for wax deposition, molecular diffusion and shear dispersion. Both methods are calculated on a volume basis of wax deposition; the rate of deposition by molecular diffusion of a wax-forming component is given by

$$V_{\text{Diff}} = \sum_{i=1}^n \frac{D_i (c_i^b - c_i^w) S_{\text{wet}} MW_i}{\delta \rho_i} \quad (5.13)$$

where  $c_i$  is the molar concentration of component  $i$  in the bulk and at the wall.  $S_{\text{wet}}$  refers to the fraction of the perimeter wetted by the current phase, and  $MW_i$  is the molecular weight of component  $i$ ,  $\rho_i$  being the density of component  $i$ . The Greek symbol,  $\delta$ , represents the laminar sublayer inside of the pipeline and is given by [1].

$$\delta = \alpha * 11.6 \sqrt{2} \frac{D}{Re \sqrt{f}} \quad (5.14)$$

The tuning parameter,  $\alpha$  is used as a thickness correction factor that is tuned to match experimental results, the values range from 0 to 100, a value of 1.00 was used in this study. The term  $D_i$  in Equation 5.8 is the diffusion coefficient of a wax-forming component, and is calculated by the following correlation [8].

$$D_i = \beta \times 13.3 \times 10^{-12} \times T^{1.47} \mu_b \left( \frac{10.2}{\left( \frac{MW_i}{\rho_i} \right)} \right)^{-0.791} \left( \frac{MW_i}{\rho_i} \right)^{-0.71} \quad (5.15)$$

The diffusivity also contains a tuning parameter,  $\beta$ , used to fit experimental data. The value can be set from 0 to 100; the value used in this study was 1.2.

### 5.4.2 Deposition of wax by shear dispersion

Deposition by shear dispersion is calculated on a volume basis. The rate of deposition is calculated from the correlation of Burger [4] discovered.

$$V_{Shear} = \frac{k^* C_{wall} \gamma A}{\rho_{wax}} \quad (5.16)$$

where  $C_{wall}$  is the volume fraction of deposited wax at the wall,  $\gamma$  is the shear rate at the wall,  $A$  is the area available for wax deposition and  $\rho_{wax}$  is the average density of wax in the bulk phase. The constant  $k^*$  is the shear dispersion constant. This is a tuning parameter used to match experimental results. The value can be set between 0 and  $0.0001 \text{ g/cm}^2$  (0 to  $0.025 \text{ lb/ft}^2$ ). This can be set low because wax deposition due to shear dispersion has been considered negligible [4, 8] and in this study it was set at  $1 \times 10^{-9}$ .

## 5.5 Input of experimental data into PVTsim and DepoWax

The experimental measurements previously discussed in Chapter 4 also play a role in the modeling of the pipeline. For each of the physical properties measured experimentally the oils and diluent must be created in PVTsim, before it can be used in DepoWax. To create the three fluids in PVTsim the carbon number distribution of each of the fluids had to be put in. Creating the new fluids was completed by selecting “Enter New Fluid” under the fluid tab. Once this input was selected a box popped up. This box allowed for the carbon number distribution to be input for each of the fluids. Since the carbon number distribution was done by HTGC the weight fraction box was selected when entering the values for each carbon number. This was completed for all three of the fluids. Once the fluids were created the mixtures had to be created as well. Using “Mix” under the fluid tab made this possible. This allowed for the waxy oil to be mixed with



the diluent and the light crude oil in the previously mentioned weight fractions. After the mixtures were created the rheological data could then be entered for the waxy oil and diluent mixtures that were made and measured analytically. When entering the rheology data for each fluid the viscosity measurement is input for each fluid above the WAT. Once below the WAT the shear rate is input for the range of temperatures. The final characteristic that was added to each of the analytically measured fluids was the actual WAT measured.

## **CHAPTER 6**

### **RESULTS OF MODELING AND CONCLUSIONS**

#### **6.1 Description of the model**

The waxy crude oil pipeline runs from extraction point to the refinery where it can be refined into products. The diameter of the pipeline is 10" (0.254 m) with a wall thickness of 0.5" (0.0127 m) made out of cast iron with a thermal conductivity of 28.881 BTU/hr ft °F (50009 mW/m °C), constant provided by DepoWax. Other inputs used that are important to the modeling include the thermal conductivity of the wax, the roughness of the wax and the three tuning parameters mentioned in Chapter 5. The thermal conductivity of the wax was a default value from DepoWax, 0.145 BTU/hr ft °F (251.072 mW/m °C). The wax roughness value used was the same roughness value used for asphalt dipped cast iron pipe [4], 0.0004 ft (0.0001 m). The flow modeling consisted of two cases both being different. In the first the waxy crude oil was mixed with the diluent and in the second it was mixed with the light crude oil. For both of these cases the target flow rate was 40,000 bbl/day. Figure 6.1 shows a cross-sectional view of the path that the proposed pipeline follows as well as a temperature profile for the flow. The pipeline modeled is for an above ground pipeline. It also shows the location of the booster stations used along the pipeline to get the oil to the refinery.

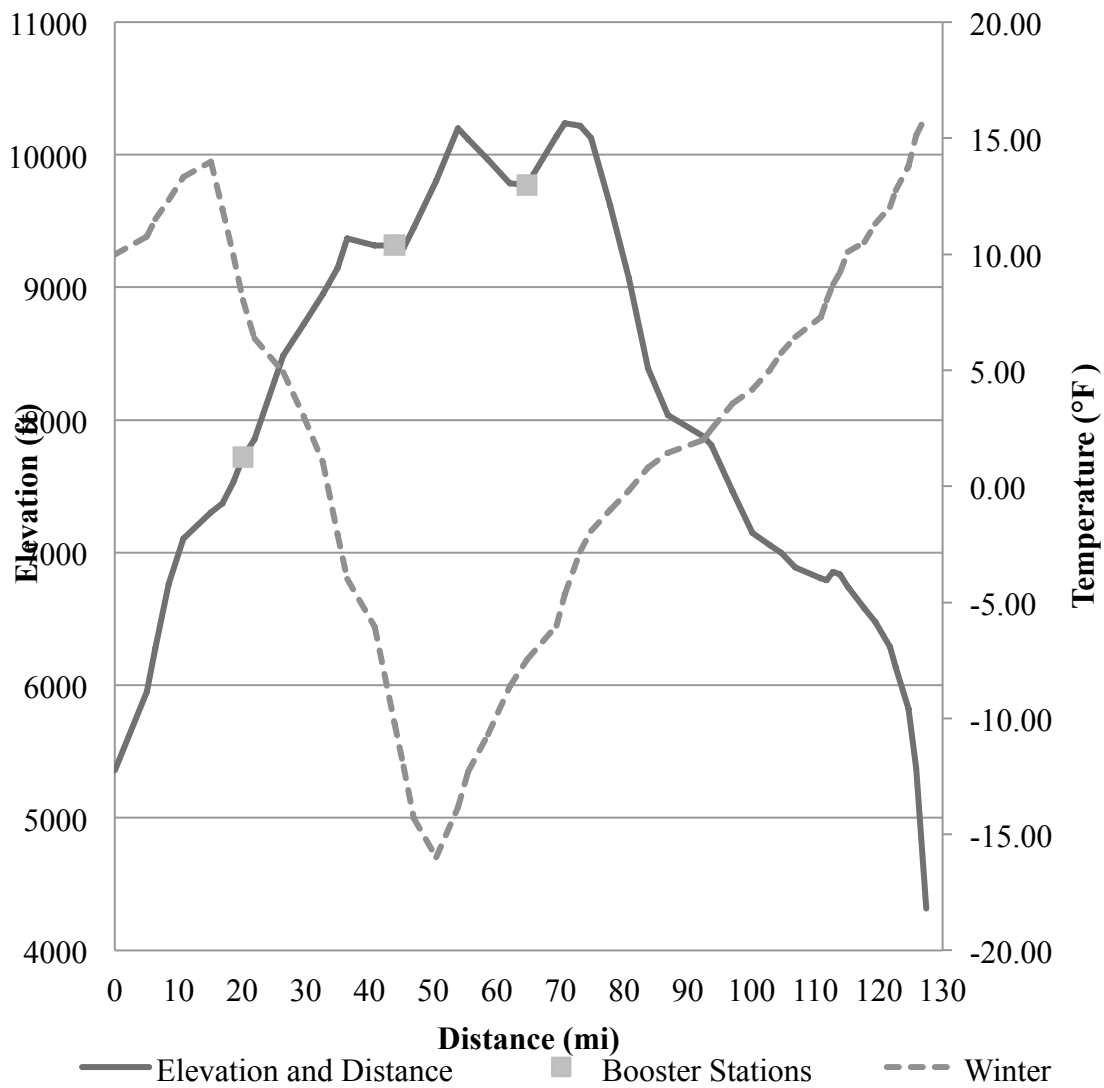


**Figure 6. 1** Cross-sectional elevation map and temperature profile for the pipeline

## 6.2 Case one waxy oil and diluent mixture

The modeling for the waxy oil and diluent mixtures will be presented in this section. The simulations were completed for cold weather. The cold weather was chosen because the possibility for deposition was at its highest due to the large temperature gradient of the oil and the ambient air. The results of the waxy oil with no diluent up to the waxy oil mixed with 50% by weight diluent are shown in increasing order from

Figure 6.2 to Figure 6.5. For each of the cases modeled the inlet temperature remained the same at 140 °F, this was done to have the oil enter the pipeline well above the WAT. The inlet pressure and the pressures at each of the booster stations varied for each of the cases in which the diluent was added and for the case where it was not added. The pressure was varied due to the decreasing viscosity of the oil with the different amounts of diluent added. The pressures are summarized in Table 6.1 to Table 6.4.

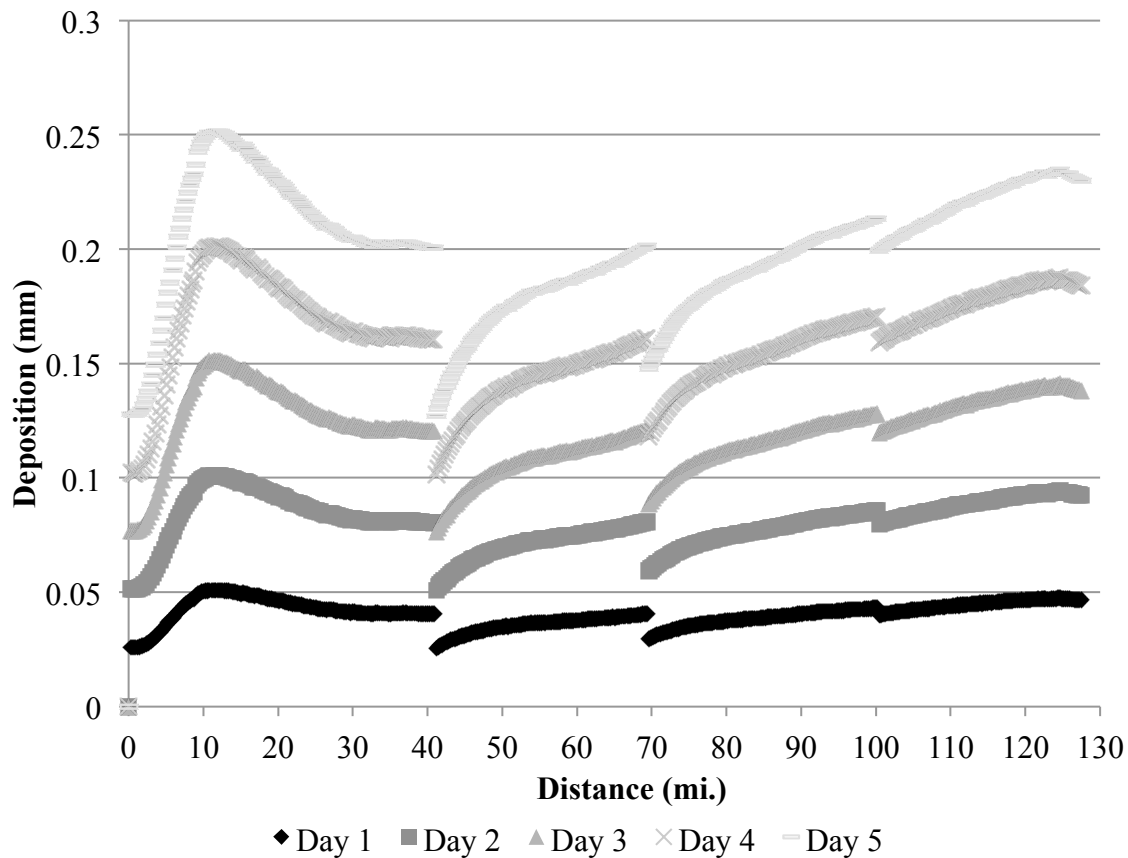


**Figure 6.2** Deposition of the waxy oil with no diluent addition.

**Table 6.1** Inlet pressure and the pressures of the booster stations for the waxy oil with no diluent added.

Inlet	16,000 PSI
Booster One	8,000 PSI
Booster Two	5,000 PSI
Booster Three	1,000 PSI

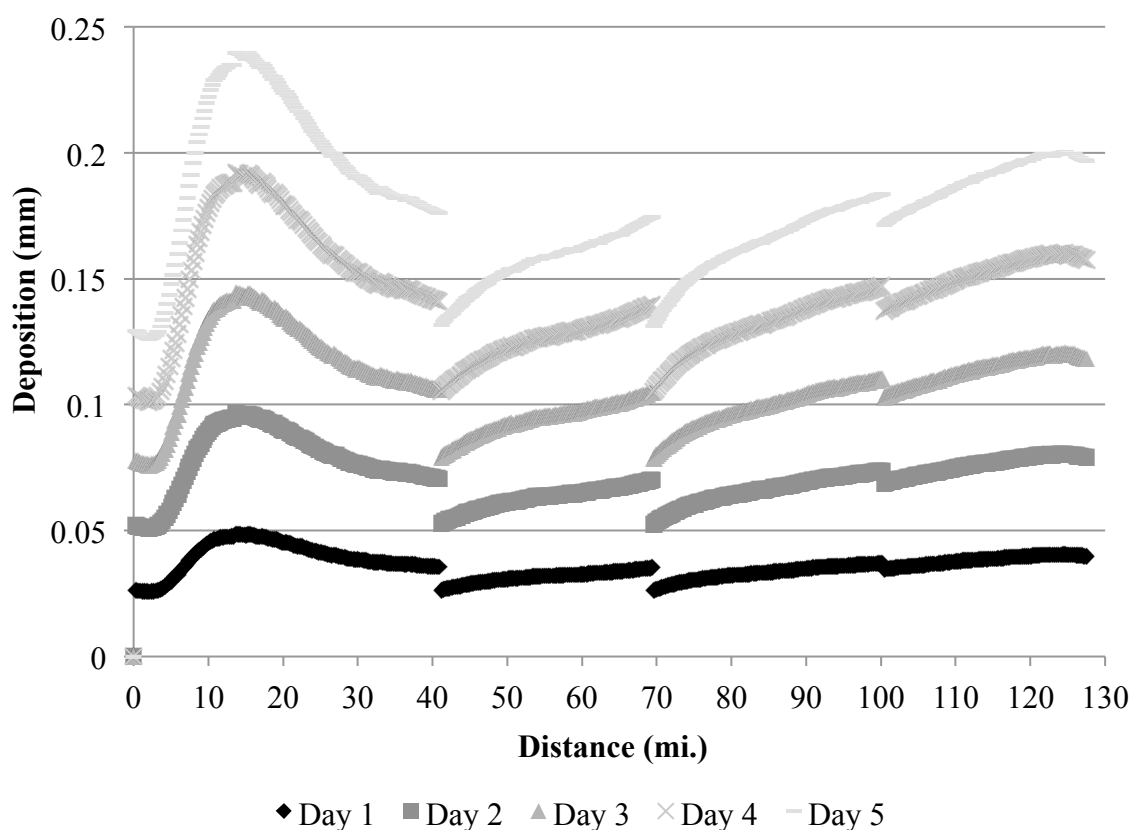


**Figure 6.3** Deposition of the waxy oil and 10% by weight diluent mixture.

**Table 6.2** Inlet pressure and the pressures of the booster stations for the waxy oil and 10% by weight diluent added.

Inlet	14,000 PSI
Booster One	5,000 PSI
Booster Two	4,500 PSI
Booster Three	1,000 PSI

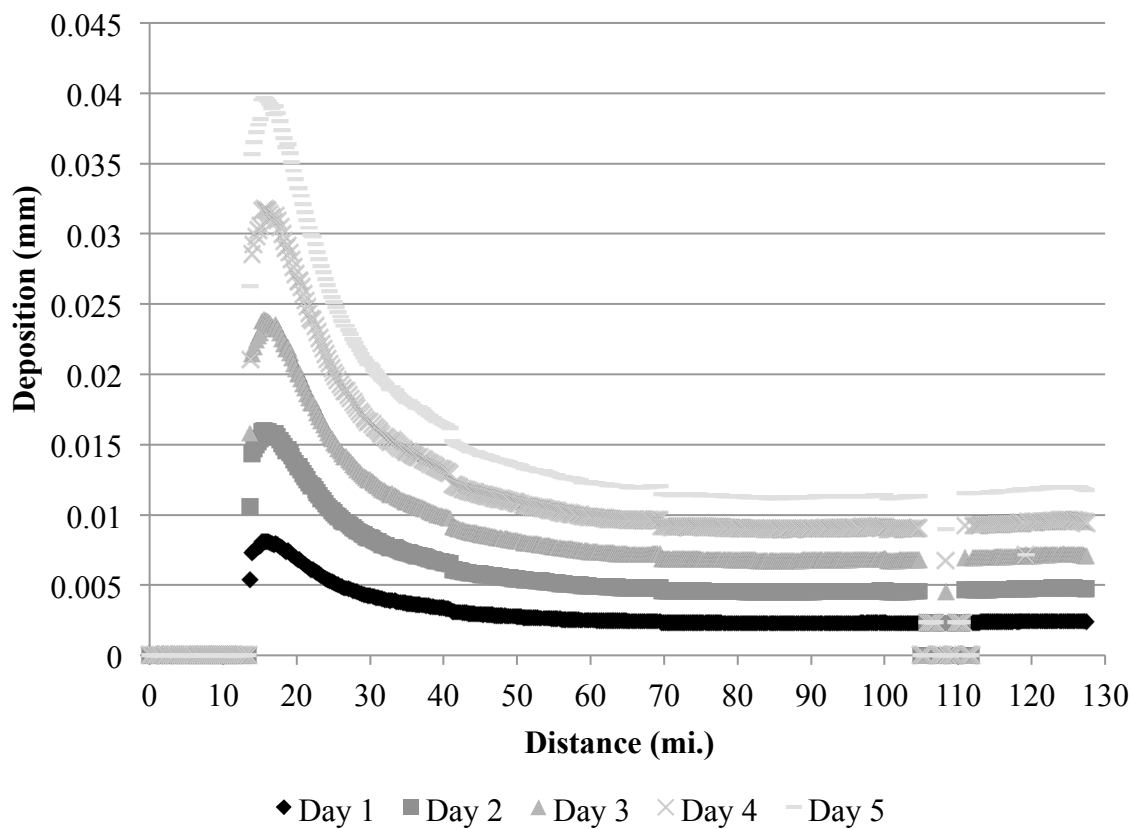


**Figure 6.4** Deposition of the waxy oil and 30% by weight diluent mixture.

**Table 6.3** Inlet pressure and the pressures of the booster stations for the waxy oil and 30% by weight diluent mixture.

Inlet	14,000 PSI
Booster One	5,000 PSI
Booster Two	4,500 PSI
Booster Three	1,000 PSI

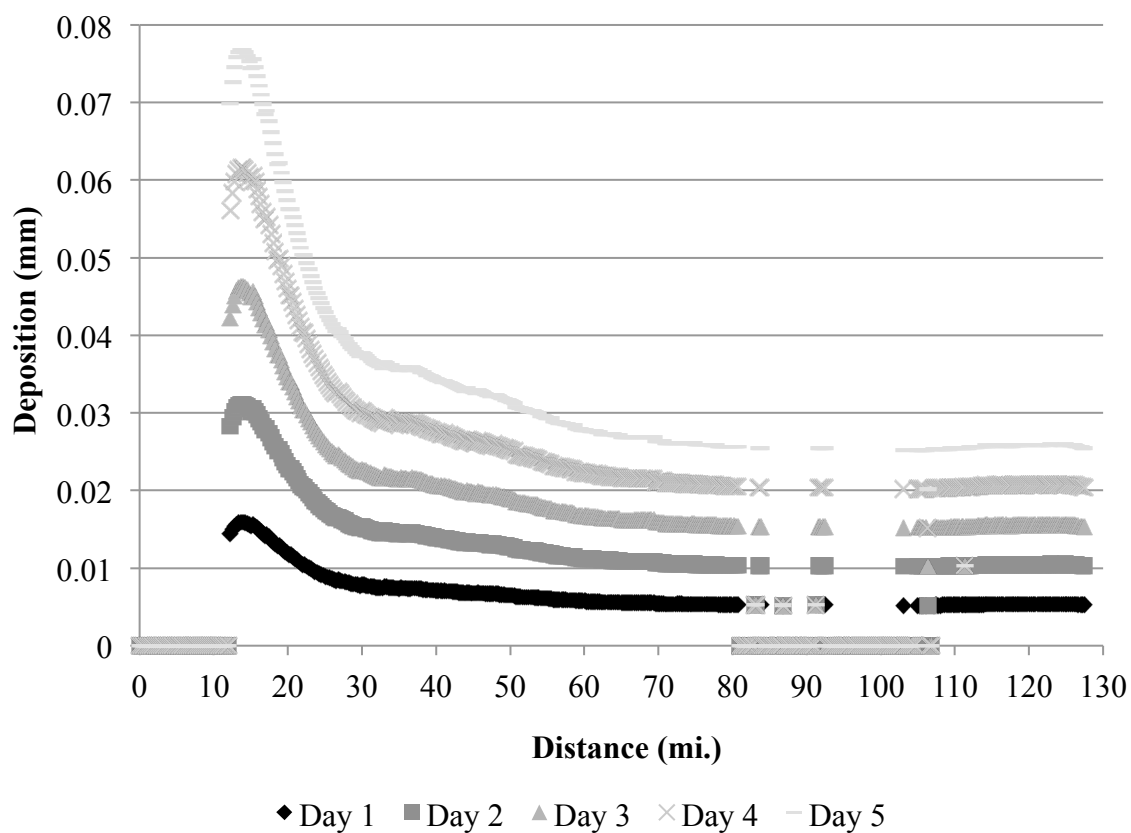


**Figure 6.5** Deposition of the waxy oil and 50% by weight diluent mixture.

**Table 6.4** Inlet pressure and the pressures of the booster stations for the waxy oil and 50% by weight diluent mixture.

Inlet	7,000 PSI
Booster One	500 PSI
Booster Two	400 PSI
Booster Three	200 PSI

### **6.3 Discussion of waxy oil and diluent mixture**

The modeling of the waxy oil mixed with diluent showed a decrease in deposition with increasing amount of diluent, with the no diluent addition case showing the largest deposition in case one. The deposition is shown to increase with each passing day; this is because wax is deposited on top of the previous day's deposition from the flowing oil. The 10% by weight diluent mixture shows a slight decrease from the waxy oil alone. The 30% by weight and 50% by weight both show the largest decrease in wax deposition. While the 30% by weight mixture shows a lower deposit thickness than the 50% by weight mixture. However the 50% by weight mixture does have a long stretch of pipeline that exhibits no deposition.

### **6.4 Case two waxy oil and light crude mixture**

This section presents the results of the waxy oil mixed with the light crude oil. The simulations were also completed when the weather is cold. The mixtures follow the same pattern as the mixtures in case one. The mixtures are the light crude only, 10% by weight waxy oil, 30% by weight waxy oil and 50% by weight waxy oil. The inlet temperature of the mixtures is the same as it was in case one, 140 °F. The results of the deposition modeling are shown in Figure 6.6 to Figure 6.10. The inlet pressures and the booster station pressures are also summarized in Table 6.5 to Table 6.9.



**Table 6.5** Inlet pressure and the pressures of the booster stations for the light crude with no waxy oil added.

Inlet	5,000 PSI
Booster One	500 PSI
Booster Two	400 PSI
Booster Three	200 PSI

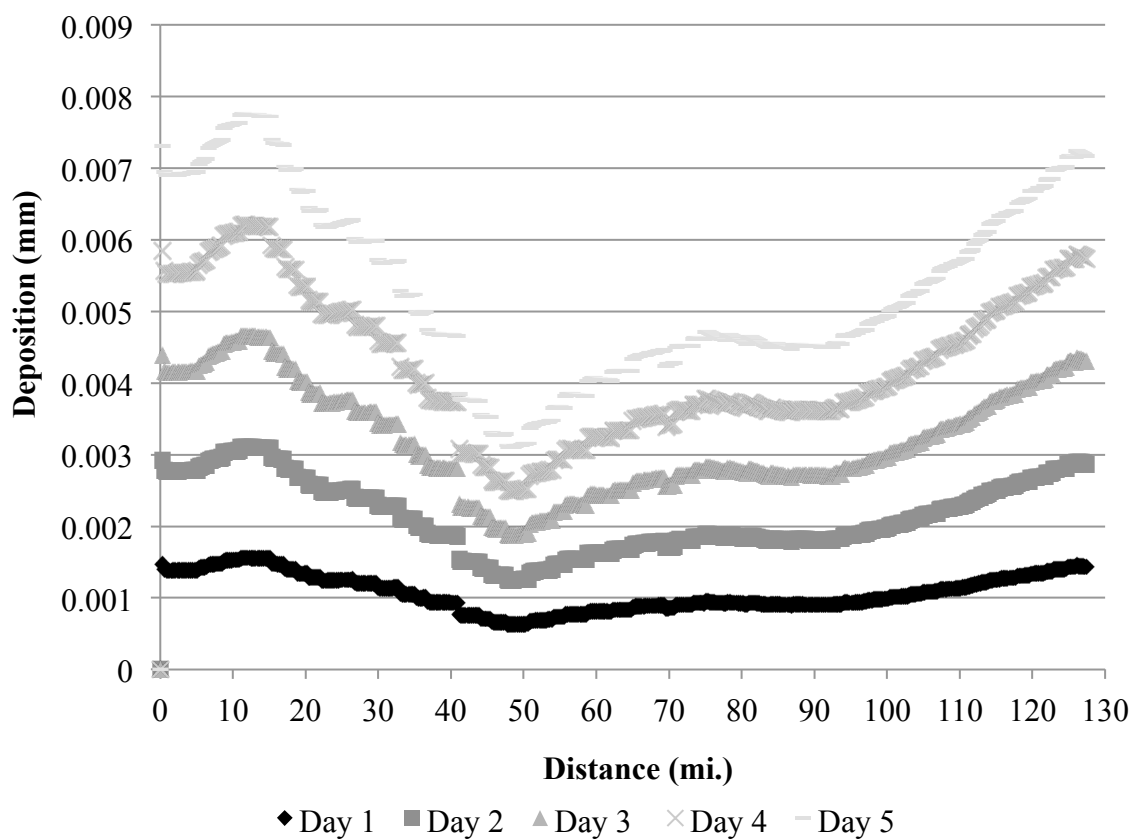


**Figure 6.6** Deposition of the light crude oil with no waxy oil added.

**Table 6.6** Inlet pressure and the pressures of the booster stations for the light crude and 10% by weight waxy oil mixture.

Inlet	9,000 PSI
Booster One	500 PSI
Booster Two	400 PSI
Booster Three	200 PSI

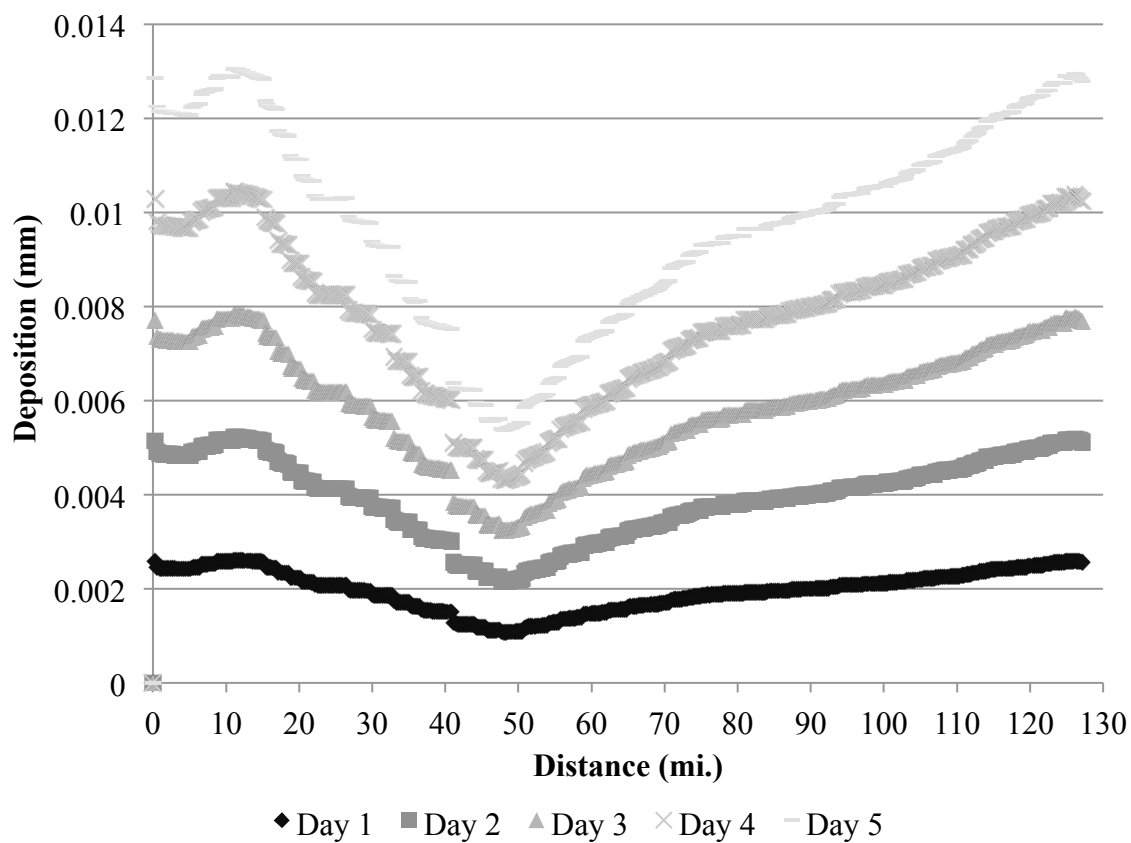


**Figure 6.7** Deposition of the light crude oil with 10% by weight waxy oil added.

**Table 6.7** Inlet pressure and the pressures of the booster stations for the light crude and 30% by weight waxy oil mixture.

Inlet	10,000 PSI
Booster One	500 PSI
Booster Two	400 PSI
Booster Three	200 PSI

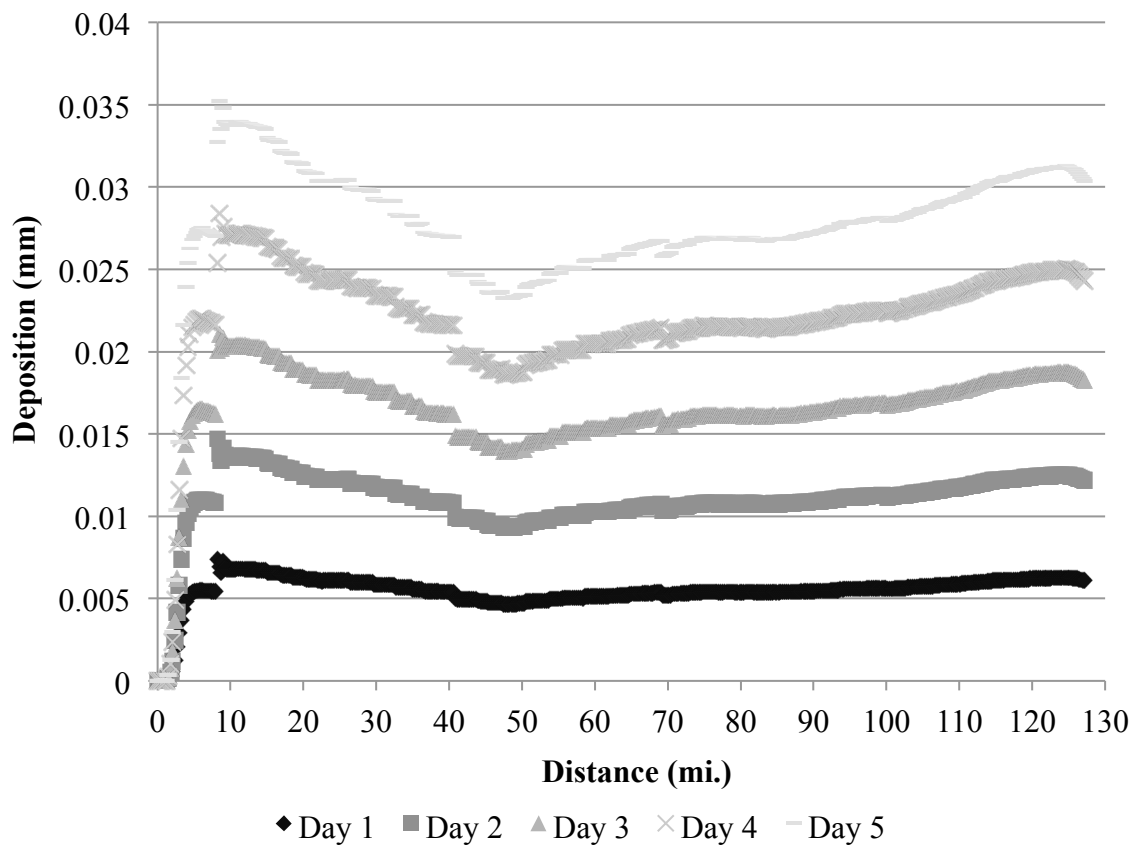


**Figure 6.8** Deposition of the light crude oil with 30% by weight waxy oil added.

**Table 6.8** Inlet pressure and the pressures of the booster stations for the light crude and 50% by weight waxy oil mixture.

Inlet	12,000 PSI
Booster One	500 PSI
Booster Two	400 PSI
Booster Three	200 PSI

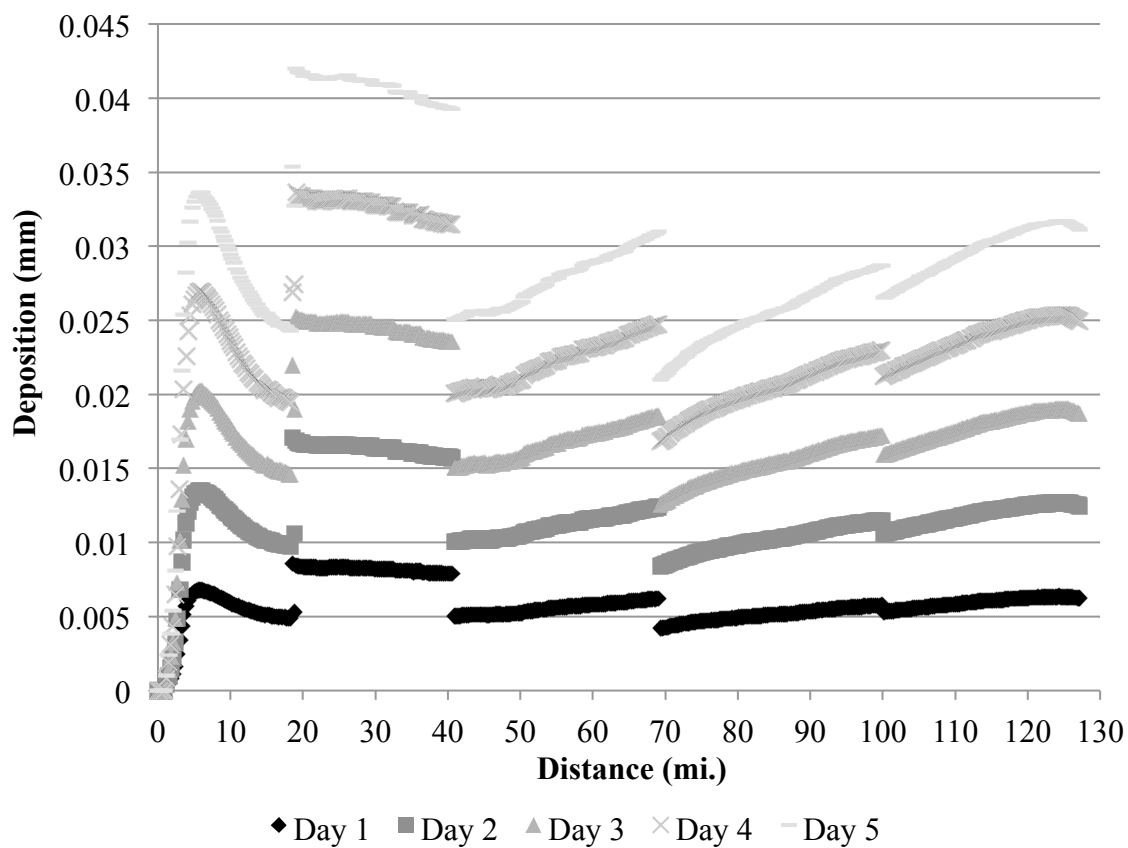


**Figure 6.9** Deposition of the light crude oil with 50% by weight waxy oil added.

### **6.5 Discussion of light crude and waxy oil mixture**

The second case where the black wax is mixed with the light crude oil shows a lower amount of deposition than that of case one. The models show that as the percent of black wax mixed with the light crude increases the deposition increases, with the 50% by weight black wax and light crude showing the largest amount of deposition for case two. The light crude oil alone does show deposition. Deposition is shown for the light crude alone because there are still carbon numbers above C18, although not as many when compared to the black wax, which are paraffins that lead to the deposition in the second case.

### **6.6 Conclusions**

The simulations show that the deposition for case two will result in a lower amount than that for case one. However to get the light crude oil the company pumping the waxy crude oil would need to purchase some of the light crude to blend with the waxy crude oil. The light crude oil could be blended near the beginning of the pipeline; this would not require the light crude oil to be transported by other means, other than another pipeline, which could already be in place. In the case of the diluent, it would need to be transported in from a refinery, since it is a light fractional distillate from the crude oil. Using the simulations of the pipeline deposition also aids in a maintenance schedule of the pipeline for both of the cases. The simulations allow a proactive approach to keep the pipeline from being plugged and then possibly having to abandon an entire section or large costs associated with removing the plug in the pipeline.

The recommendation for the waxy oil and diluent mixture is 30% by weight diluent. While this does not entirely stop the deposition it does hinder it. In this case there also is the possibility of recovering the diluent at the refinery as well as getting more from the fraction that is the waxy crude oil resulting in a possible excess of diluent that could be transported back to the start of the pipeline.

For the case of the waxy oil mixed with the light crude oil the 50% by weight mixture would be recommended, as it shows the lowest amount of deposition for the second case. The light crude oil would also be more readily available due to the current pipeline pumping the light crude oil.

The pumping pressure for the two cases is quite large. The reason for the pressure being so large is due to the large temperature gradient between the oil and the outside air. The oil would cool below the WAT for both cases quite rapidly during flow, causing an increase in deposition and a larger pressure gradient required to continue flow in the pipeline.

Overall when the two cases are compared the waxy crude oil with diluent addition shows that a lower overall deposition throughout the whole pipeline will decrease. The light crude does show a decrease in deposition and then begins to increase, as the pipeline gets closer to the refinery. From the simulations the case of the diluent addition appears to be the best for the case of reducing pipeline deposition and ensuring flow. However to determine which case would be the most feasible, an economic study would need to be completed.

## APPENDIX

### FLASH OUTPUT FROM PVTsim

Table A.1 to Table A.8 show the physical properties of each of the oils used in the simulation. The flash capability of PVTsim was used to do this. All the flashes were completed at 60 °F and 14.65 psia. The flashes were performed in order of increasing diluent, from the black wax only to the 50% by weight diluent mixture shown in Table A.1 to Table A.4. The second set of flash calculations were performed in order from light crude oil only to 50% by weight waxy oil added and are shown in Table A.5 to Table A.9.

**Table A.1** Flash output for the waxy crude oil.

Property	Value	Units
Volume	6.57	ft <sup>3</sup> /lb-mol
Density	55.4767	lb/ft <sup>3</sup>
Z Factor	0.0173	---
Molecular Weight	364.39	---
Enthalpy	-46840.1	BTU/lb-mol
Entropy	-39.56	BTU/lb-mol °F
Heat Capacity (Cp)	166.01	BTU/lb-mol °F
Heat Capacity (Cv)	160.22	BTU/lb-mol °F
Kappa (Cp/Cv)	1.036	---
Thermal Conductivity	0.053	BTU/hr ft °F

**Table A.2** Flash output for the 10% by weight diluent mixture.

<b>Property</b>	<b>Value</b>	<b>Units</b>
Volume	5.12	ft <sup>3</sup> /lb-mol
Density	54.0575	lb/ft <sup>3</sup>
Z Factor	0.0134	---
Molecular Weight	276.58	---
Enthalpy	-36566.0	BTU/lb-mol
Entropy	-32.58	BTU/lb-mol °F
Heat Capacity (Cp)	127.95	BTU/lb-mol °F
Heat Capacity (Cv)	122.07	BTU/lb-mol °F
Kappa (Cp/Cv)	1.048	---
Thermal Conductivity	0.077	BTU/hr ft °F

**Table A.3** Flash output for the 30% by weight diluent mixture.

<b>Property</b>	<b>Value</b>	<b>Units</b>
Volume	3.64	ft <sup>3</sup> /lb-mol
Density	53.8755	lb/ft <sup>3</sup>
Z Factor	0.0096	---
Molecular Weight	196.04	---
Enthalpy	-28035.3	BTU/lb-mol
Entropy	-28.09	BTU/lb-mol °F
Heat Capacity (Cp)	88.91	BTU/lb-mol °F
Heat Capacity (Cv)	82.83	BTU/lb-mol °F
Kappa (Cp/Cv)	1.073	---
Thermal Conductivity	0.084	BTU/hr ft °F



**Table A. 4** Flash output for the 50% by weight diluent mixture.

<b>Property</b>	<b>Value</b>	<b>Units</b>
Volume	2.88	ft <sup>3</sup> /lb-mol
Density	48.8686	lb/ft <sup>3</sup>
Z Factor	0.0076	---
Molecular Weight	140.83	---
Enthalpy	-20448.4	BTU/lb-mol
Entropy	-22.46	BTU/lb-mol °F
Heat Capacity (Cp)	68.13	BTU/lb-mol °F
Heat Capacity (Cv)	61.84	BTU/lb-mol °F
Kappa (Cp/Cv)	1.102	---
Thermal Conductivity	0.085	BTU/hr ft °F

**Table A.5** Flash output for the light crude oil.

<b>Property</b>	<b>Value</b>	<b>Units</b>
Volume	3.99	ft <sup>3</sup> /lb-mol
Density	52.7792	lb/ft <sup>3</sup>
Z Factor	0.0105	---
Molecular Weight	210.85	---
Enthalpy	-30054.7	BTU/lb-mol
Entropy	-28.58	BTU/lb-mol °F
Heat Capacity (Cp)	98.09	BTU/lb-mol °F
Heat Capacity (Cv)	91.99	BTU/lb-mol °F
Kappa (Cp/Cv)	1.066	---
Thermal Conductivity	0.074	BTU/hr ft °F

**Table A.6** Flash output for the 10% by weight waxy oil mixture.

Property	Value	Units
Volume	4.31	ft <sup>3</sup> /lb-mol
Density	53.9564	lb/ft <sup>3</sup>
Z Factor	0.0113	---
Molecular Weight	232.76	---
Enthalpy	-32273.2	BTU/lb-mol
Entropy	-31.07	BTU/lb-mol °F
Heat Capacity (Cp)	106.75	BTU/lb-mol °F
Heat Capacity (Cv)	100.73	BTU/lb-mol °F
Kappa (Cp/Cv)	1.060	---
Thermal Conductivity	0.077	BTU/hr ft °F

**Table A.7** Flash output for the 30% by weight waxy oil mixture.

Property	Value	Units
Volume	5.56	ft <sup>3</sup> /lb-mol
Density	55.5148	lb/ft <sup>3</sup>
Z Factor	0.0146	---
Molecular Weight	308.66	---
Enthalpy	-40677.8	BTU/lb-mol
Entropy	-35.11	BTU/lb-mol °F
Heat Capacity (Cp)	139.52	BTU/lb-mol °F
Heat Capacity (Cv)	133.68	BTU/lb-mol °F
Kappa (Cp/Cv)	1.044	---
Thermal Conductivity	0.070	BTU/hr ft °F

**Table A.8** Flash output of the 50% by weight waxy oil mixture.

Property	Value	Units
Volume	5.06	ft <sup>3</sup> /lb-mol
Density	54.9878	lb/ft <sup>3</sup>
Z Factor	0.0133	---
Molecular Weight	278.40	---
Enthalpy	-37327.8	BTU/lb-mol
Entropy	-33.23	BTU/lb-mol °F
Heat Capacity (Cp)	126.45	BTU/lb-mol °F
Heat Capacity (Cv)	120.54	BTU/lb-mol °F
Kappa (Cp/Cv)	1.049	---
Thermal Conductivity	0.074	BTU/hr ft °F

## REFERENCES

- [1] Bendiksen, K. H., et al. "The Dynamic Two-Fluid Model OLGA: Theory and Application." *SPE*, no. 19451, 171-180, 1991.
- [2] Bird, B. R., W.E. Stewart and E.N Lightfoot. *Transport Phenomena*. 2<sup>nd</sup> edition. New York: John Wiley and Sons, 2002
- [3] Burger, E. D., T. K. Perkins and J. H. Striegler. "Studies of Wax Deposition in the Trans Alaska Pipeline." *Journal of Petroleum Technology*, pp. 1075-1086, 1981.
- [4] Brown, T. S., V. G. Niesen and D. D. Erickson. "Measurement and Prediction of the Kinetics of Paraffin Deposition." *SPE*, no. 26548, pp. 353-368, 1993.
- [5] *Cameron Hydraulic Data 17th Edition*, Ingersoll-Rand. New Jersey, 1988.
- [6] Creek, J. L., et al. "Wax Deposition in Single Phase Flow." *Fluid Phase Equilibria*, pp. 801-811, 1999.
- [7] Dahdah, N. F. "Comparative Compositional Study of Crude Oil Solids from the Trans Alaska Pipeline System Using High-Temperature Gas Chromatography." *Energy & Fuels*, pp. 211-217, 2002.
- [8] Hamouda, A. A., and S. Davidsen. "An Approach for Simulation of Paraffin Deposition in Pipelines as a Function of Flow Characteristics With a Referene to Teesside Oil Pipeline." *SPE*, no. 28966, pp. 213-224, 1995.
- [9] Hayduk, W., and B. S. Minhas. "Correlations for Prediction of Molecular Diffusivities in Liquids." *The Canadian Journal of Chemical Engineering*, pp. 295-299, 1985.
- [10] Hunt, E. "Laboratory Study of Paraffin Depositon." *Petroleum Transactions*, pp. 1259-1269, 1962
- [11] Hsu, J.J. C., M. M. Santamaria and J. P. Brubaker. "Wax Deposition of Waxy Live Crudes Under Turbulent Flow Conditions." *SPE*, no. 28480, pp. 179-192, 1994.

- [12] Jessen, F. W., and J. N. Howell. "Effect of Flow Rate on Paraffin Accumulation in Plastic, Steel, and Coated Pipe." *Petroleum Transactions*, pp. 80-84, 1958.
- [13] Leiroz, A.T., and L. F. A. Azevedo. "Studies on the Mechanisms of Wax Deposition in Pipelines." OTC no. 17081, 1-11, 2005
- [14] Parra-Ramírez, M. J. *Precipitation and Characterization of Asphaltenes*. Ph.D. Thesis, University of Utah, 2002
- [15] Pedersen, K. S. "Prediction of Cloud Point Temperatures and Amount of Wax Precipitation." *SPE*, no. 27629, pp 46-49, 1994.
- [16] *PVTsim 19 Methodology Documentation*, Calsep International Consultants, Houston, TX, 2009.
- [17] *PVTsim Help*, Calsep International Consultants, Houston, TX, 2009
- [18] Roehner, R. M., and F. V. Hanson. "Determination of Wax Precipitation Temperature and Amount of Precipitated Solid Wax Versus Temperature for Crude Oils Using FT-IR Spectroscopy." *Energy & Fuels*, pp. 756-763, 2001
- [19] Rønningsen, H. P., and K. S. Pedersen. "Effect of Precipitated Wax on Viscosity – A Model for Predicting Non-Newtonian Viscosity of Crude Oils." *Energy & Fuels*, pp. 43-51, 2000.
- [20] *Standard Test Method for Determination of Boiling Range Distribution of Crude Petroleum by Gas Chromatography*, ASTM D 5307-97, 1997.
- [21] Weingarten, J. S., and J. A. Euchner. "Methods for Predicting Wax Precipitation and Deposition." *SPE Production Engineering*, pp. 121-126, 1988.